SCHOOL OF MINING AND GEOSCIENCES

Processing of Kazakh Red Mud (KRM) for the Selective Recovery of Rare Earth Elements (REEs) through microwave-assisted acid leaching

by

Aruzhan Yubileyeva

Thesis Supervisor

Ata Akcil

Thesis submitted to the School of Mining and Geosciences of Nazarbayev University in Partial Fulfillment of the Requirements for the Degree of Bachelor of Science in Mining Engineering

Nazarbayev University

13.04.2026

Originality statement

I, Aruzhan Yubileyeva, hereby declare that this submission is my own work and to the best of my knowledge it contains no materials previously published or written by another person, or substantial proportions of material which have been accepted for the award of any other degree or diploma at Nazarbayev University or any other educational institution, except where due acknowledgement is made in the thesis. Any contribution made to the research by others, with whom I have worked at NU or elsewhere is explicitly acknowledged in the thesis. I also declare that the intellectual content of this thesis is the product of my own work, except to the extent that assistance from others in the project's design and conception or in style, presentation and linguistic expression is acknowledged.

Signed on 17.04.2026

Acknowledgment

I would like to express my sincere and heartfelt thanks to my thesis supervisor, Professor Ata Akcil, for his invaluable guidance and support throughout this research. I am also grateful to my co-supervisor, Dr. Mert Guney, for his guidance and suggestions. I would also like to express my appreciation to the Core Facility for Chemical Analysis for providing access to advanced instrumentation and technical support essential for this research. I would like to extend my appreciation to Dr. Syed Shah for his support, valuable input, and encouragement during the course of this work. In addition, I am grateful to the Ministry of Science and Higher Education of the Republic of Kazakhstan for their financial support and assistance. Lastly, I would like to express my heartfelt thanks to my family for their support and encouragement throughout my academic career. This research was conducted under project OPCRP2025014: Technology Development of Rare Earth Metals Recovery in the Closed Cycle of Red Mud Processing.

Abstract

Bauxite residue, also known as Red Mud (RM), is generated through the Bayer Process and is considered one of the most environmentally hazardous by-products of aluminum production. It is also viewed as a secondary source of several other valuable metals, including Rare Earth Elements (REEs). However, the recovery of these REEs is hampered because they are strongly associated with various mineral phases, including iron oxide, aluminosilicate, and Ti-bearing minerals, making it difficult to extract them through conventional leaching. In this thesis, we have investigated how Microwave Assisted Pretreatment can be used to improve the Recovery of selected REEs (Ce, Nd, Sm and Eu) from Kazakhstan Red Mud (KRM) when microwave treatment was utilized in an effort to create changes at a micro level to the structure of KRM particles to disrupt the size of particles, to cause cracking within particles, and modify the mineral phases containing the REE's. Once pre-treatments had been completed, leach solutions were prepared utilizing various types of acidic media under controlled experimental conditions. Both treated and untreated samples were analyzed using X-Ray Diffraction (XRD), X-Ray Fluorescence (XRF), Scanning Electron Microscopy/Energy Dispersive Spectroscopy (SEM/EDS), and Fourier Transform InfraRed Spectroscopy (FTIR) in order to assess changes in the mineral composition and structural properties of KRM. The obtained results demonstrated that microwave-assisted pre-treatment significantly improved leaching yields over those obtained directly via leaching. We also found that the primary mechanisms responsible for this enhancement included increased structural disruption in KRM, resulting in better access for the leaching agent into the solid phase. Of note, significant enhancements in the leaching of Ce and Nd occurred, however, Sm and Eu showed minimal enhancement in leaching due to their association with more stable mineral phases.

Table Contents

List of Figures

List of Tables

1. Introduction

1.1 Background

Red Mud (RM) or bauxite residue refers to an alkaline particulate material generated during Bayer digestion, the process used to create aluminum oxide to produce alumina, as illustrated by Figure 1. Approximately 1–2 tons of RM are created per ton of aluminum oxide produced for all alumina producers around the world. The RM has many characteristics that make it difficult to manage, such as alkalinity, high sodium content, and its complicated composition of minerals (iron oxides, aluminosilicate minerals, titanium-containing minerals, desilication products, and amorphous components), as well as its fine particle size. It is also very absorbent and, therefore, difficult to work with. As a result of these attributes, conventional methods of disposing of this type of waste include depositing it in "tailings" lakes and/or piling it in dry mounds. Both of these types of disposition require considerable areas of land and continual monitoring over many years. Neither method provides any assurances of preventing long-term environmental consequences resulting from the leaching of alkali from the red mud into waterways and the creation of dust, unstable structures, etc. (Wang et al. 2019; Evans 2016; Çelebi 2024; Swain, Akcil, and Lee 2022; Akcil et al. 2024).

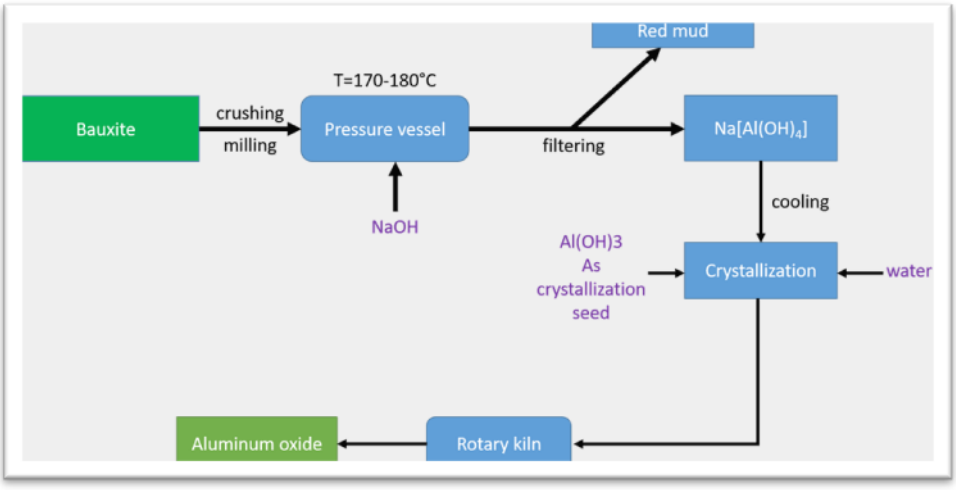

Figure 1. Simplified flow diagram of the Bayer process for alumina production, showing bauxite digestion, red mud separation, and aluminum hydroxide precipitation.

Recent developments concerning the environment have changed public perceptions of RM from being viewed as waste materials to a possible secondary resource. The studied KRM sample contains large amounts of Fe, Al, Ti, and Na, along with small quantities of other important rare earth metals (REEs). REEs are very important to current technology and could be an excellent source for the extraction of some of the most important components required by high-tech manufacturing. However, extracting the REEs from RM is difficult because they are located inside solid minerals like iron oxide and aluminosilicate minerals. This makes them hard to access when they go through the traditional leaching process. As a result, there has been a great deal of interest in new techniques that will help to alter the structure of the minerals and allow for better extraction. Microwave-assisted pretreatment is one of those techniques; microwave heat creates local hot spots and forms micro-cracks in the minerals while also creating phase transformations. It increases the diffusion in the minerals and releases the embedded elements (Al-Harahsheh and Kingman 2004; Amankwah, Pickles, and Yen 2005; Liu et al. 2020; Singh et al. 2019).

In this study, the Kazakh Red Mud (KRM) sample was studied, which was taken from the Pavlodar Aluminum plant in Kazakhstan, after undergoing controlled thermal processing at industrial temperatures and conditions. The purpose of this research project was to investigate the effects of microwave pre-treatment on the extraction of certain REE's (Ce, Nd, Sm, and Eu) using two different acidic systems, as well as determine if structural or mineralogical changes affected the extraction.

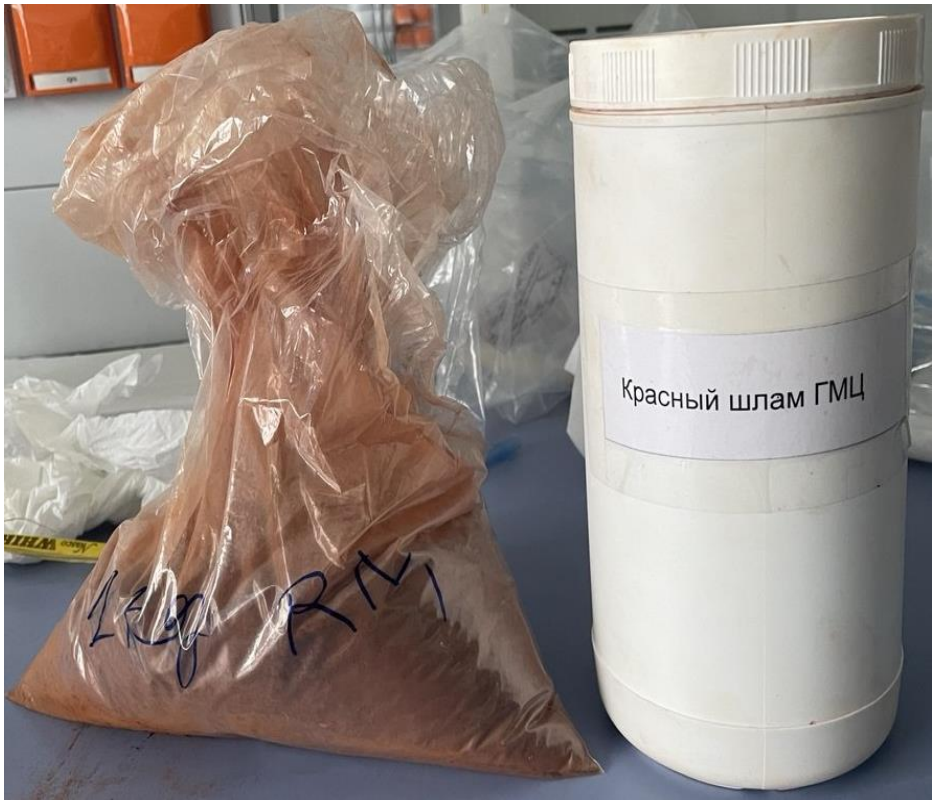

Figure 2. Red mud powder sample used in this study.

1.1.1 Bauxite as the Primary Ore for Aluminium Production

Bauxite provides the main source of alumina (Al_2O_3), as well as the major raw material from which all forms of aluminium are manufactured. Typically, bauxite contains a range of aluminum-bearing minerals including gibbsite ($Al(OH)_3$), boehmite (γ-AlO(OH)), and diaspore (α-AlO(OH)). Iron oxides and silicate phases, along with titanium minerals such as anatase and rutile, commonly occur in bauxites. Because bauxites form under many different geological conditions and undergo many types of weathering before they are mined, bauxites exhibit a wide range of compositions. Variations in the composition of bauxites affect both the processes used to extract alumina from them and the physical/chemical characteristics of the resulting RM. As an example, bauxites that contain high levels of gibbsite can be processed by Bayer processing, while those containing higher levels of diaspore or silica will need to be treated at more extreme temperatures (e.g., elevated temperature digestion/sintering). In addition to affecting how efficiently alumina can be extracted, the proportion of key oxide components (Fe_2O_3, SiO_2, CaO, Na_2O, and TiO_2) in bauxites determines the mineralogy of RM. Consequently, the variability in bauxite composition results in varying RM properties. Ultimately, these property differences impact the reaction and processing behavior of RM during leaching (Du et al. 2024; Wang et al. 2019).

1.1.2 Formation and Composition of Red Mud

Bauxite residue or RM is a non-soluble byproduct of the Bayer Process for extracting aluminum from bauxite. Aluminum-bearing minerals dissolve in NaOH, but iron oxides, titanium-containing mineral phases, silica-rich minerals, and undissolvable compounds remain. Washing and separating after dissolution results in RM, which is usually produced in volumes of 1-2 tonnes per tonne of alumina. The reddish tint of RM is primarily due to iron oxide presence including Hematite and Goethite.

RM has a complex and very heterogeneous composition. RM's primary composition includes iron oxides (wt% approximately 30-60%) and aluminosilicates, titanium oxides (anatase, rutile, etc.), desilication products, and a significant amount of amorphous phase that forms during digestion. Additionally, remaining NaOH and Na-containing minerals (sodalite, cancrinite, etc.) result in

RMs high alkalinity levels with pH values > 12. Due to its low particle size, multiple-phase composition, and strong alkaline nature, RM presents problems regarding storage and handling. Further, it influences RM's reactivity and performance during metals extraction processes (Wang et al. 2019; Du et al. 2024). Typical SEM-EDS analyses demonstrate the close association of iron-rich, aluminosilicate, and titanium-containing phases throughout RM's particle structures and elemental distributions. The heterogeneous particle morphology and multi-phase elemental distribution of RM are illustrated in Figure 3, which shows typical SEM and EDS maps highlighting the intimate association of Fe-oxide, aluminosilicate, and Ti-bearing phases

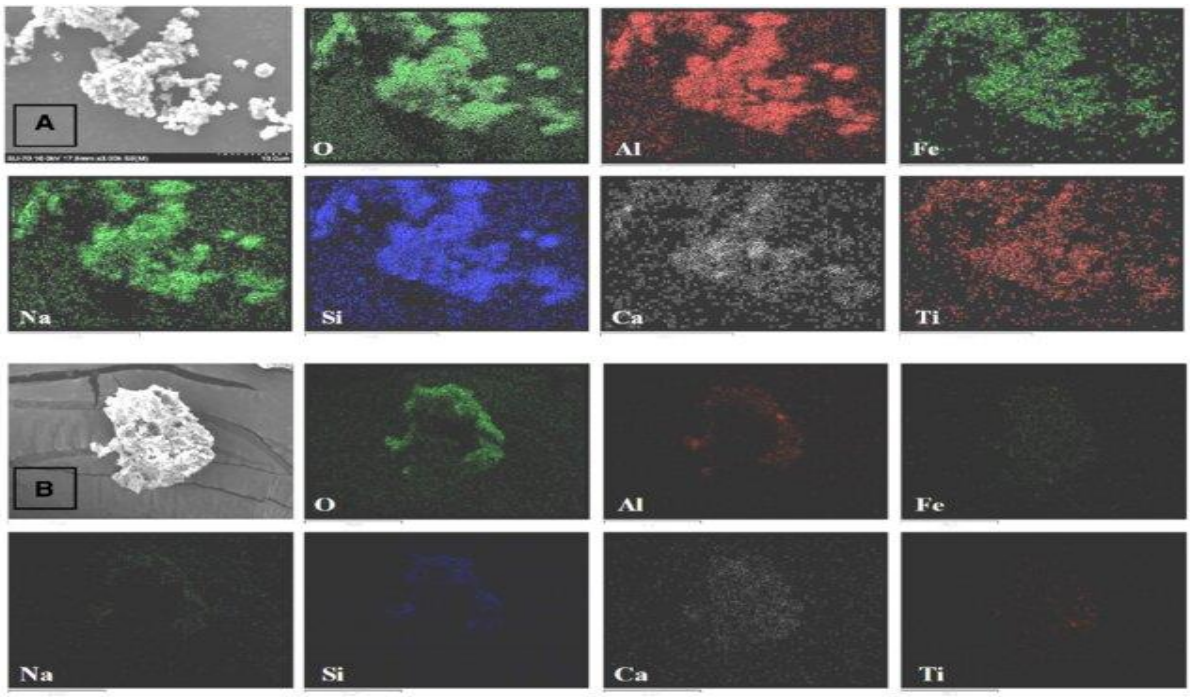

Figure 3. SEM images and corresponding EDS elemental maps of RM sample. Image (A) shows a heterogeneous agglomerate with distinct distributions of O, Al, Fe, Na, Si, Ca, and Ti, while image (B) illustrates a smaller particle with lower elemental signal intensity. The maps highlight the heterogeneous distribution of major elements and the close association of iron-rich, aluminosilicate, and titanium-bearing phases within the RM matrix.

1.2 Environmental, Operational, and Economic Challenges of RM Disposal

1.2.1 Operational and Engineering Challenges

The primary source of operational issues with respect to managing RM is largely attributed to the extremely small diameter of individual particles and their high surface area, along with the colloid nature of these materials. The combination of these factors results in difficulties in separating liquid from solids in dewatering processes and subsequently results in slow settling and consolidation rates. Consequently, large holding tanks in the form of settling ponds or thickeners are typically used to store RM. Additionally, many times chemicals referred to as flocculants are added to the system to aid in improving solid-liquid separation. The increased need for large storage tank space also increases operational costs, since the cost of acquiring land, building dams,

controlling seepage into the dams, and monitoring the dams over extended periods of time requires significant investments (Evans 2016; Wang et al. 2019; Swain, Akcil, and Lee 2022; Du et al. 2024).

Additionally to operational concerns, there are serious environmental implications involved in storing RM. An example of this was the Ajka Alumina Plant accident in Hungary. Approximately 1 million cubic meters of very alkaline slurry escaped when the dam failed. This incident illustrated several types of risks that can be caused by mismanaging RM, including the contamination of soil and water resources and potential structural instability problems associated with sludge rheology. There have been numerous similar accidents around the world, and it has become apparent that such accidents do occur (Evans 2016; Swain, Akcil, and Lee 2022; Du et al. 2024). In addition to the risk associated with structural collapse, RM may present environmental hazards even while being managed within acceptable parameters. For instance, during periods of drought, dry climates generate dust emissions. During periods of heavy rainfall or overflow, RM's fine alkaline particulate matter will disperse in the environment. These environmental and operational challenges highlight the necessity for effective RM management methods and have generated an increase in interest toward developing alternative methods to manage RM in order to minimize storage volume and environmental impacts associated with managing RM.

Figure 4. Environmental hazards and management practices associated with RM, large-scale storage, spill incidents, and potential dispersion of alkaline material (Ruyters et al. 2011).

1.3 Economic Considerations

Globally, an estimated 150-175 million tonnes of RM are produced annually (Li. Z. 2026). The stockpiled amount exceeds four billion tonnes. Impoundments for these materials usually take up acres of land and therefore require constant investment in the infrastructure needed to support them, e.g., dam construction, controlling seepage, managing dust, etc. Long-term monitoring systems will be required. Because every tonne of aluminium oxide (alumina) produces 1-2 tonnes of residue, even the smallest alumina refineries generate considerable quantities of RM over their lifespan; thus presenting both environmental and economic concerns.

RM Management Costs are sizeable with estimates at $4-$10 per tonne. During the lifetime of an alumina refinery, this can lead to hundreds of millions of dollars. At a global level, the cumulative financial burden of storing, maintaining, and rehabilitating all RM disposal sites will be enormous. Therefore, in addition to rising costs due to increased regulatory requirements concerning environmental protection and reduced availability of land for use as disposal facilities, there has been an increase in interest regarding the development of alternative methods for RM management. Specifically, valorisation strategies focused on metal recovery offer the potential to reduce storage volumes, lower long-term costs, and transform RM from a waste material into a valuable secondary resource (Evans 2016; Wang et al. 2019).

1.4 Emerging Perspective of RM as a Strategic Secondary Resource

1.4.1 Multi-metal Potential

In addition to the main materials found in red mud (iron oxides, aluminum, titanium, and sodium), there are many other beneficial REEs types. This fact has created increased interest in utilizing RM as a secondary source of useful materials. Typical reported total REE content levels in RM range from about 500-1700 ppm (0.05 – 0.17 weight %). Concentration ranges of scandium have been reported at up to 130-390 ppm (Akcil et al. 2024). Distribution of REEs in RM is usually controlled by Light Rare Earth Elements (LREE), however Yttrium and Scandium typically represent a smaller portion of the REEs, and Heavy Rare Earth Elements (HREE) typically represent much less of the REE (Çelebi 2024).

From an analytical/structural aspect, the REE in RM are commonly found in association with phosphate, carbonate, and titanate phases, such as Monazite, Xenotime, Synchysite, and/or as amorphous aluminosilicates in iron oxide matrices (Akcil et al. 2024; Vind et al. 2018). These associations make the REE difficult to extract because the REE are typically fine particle sizes and are structurally embedded in the matrix as opposed to being separate, discrete particles that can be

easily separated. Although the concentration levels of REE are typically lower than those of primary REE Ores, due to the high volumes of red mud produced globally, this represents a significant potential secondary source of these elements. Red Mud is now increasingly viewed through Circular Economy Frameworks as a strategic Material for the recovery of Critical Metals, specifically due to increasing pressure on supply chains and increasing demands for Sustainable Resource Utilization (Wang et al. 2019; Borra et al. 2016).

1.4.2 Alignment with Circular Economy and Resource Efficiency Goals

Beginning with the emphasis on transitioning to a circular economy through minimizing waste creation, maximizing resource efficiency, and reusing or recovering value-added products from industrial by-product material streams. In addition to utilizing alternative (circular) strategies to reduce dependence on primary natural resources through increased recycling and reuse of secondary resources versus the traditional "take-make-dispose" linear approach, there has been increasing recognition that many industrial residuals (such as RM) have high levels of recoverable material content (Evans 2016; Wang et al. 2019).

In alignment with the above circular economy objectives, the RM valorization process utilizes one of the most common waste reduction methods available today for the conversion of a voluminous waste product into a useful feedstock to allow metal and/or additional valuable materials to be recovered. Additionally, while converting large volumes of RM into usable feedstocks can eliminate the need to store them for extended periods of time, which will help minimize their negative impact on the environment, they will also contribute to conserving usable resources and improve the economic viability of both mining and processing operations. Furthermore, through the recovery of iron, aluminum, titanium, and rare earth elements contained within RM, the development of longer term sustainable, and diversified supply chain options for critical materials will be facilitated (Swain, Akcil, and Lee 2022), thus RM valorization is seen as an essential component in reaching our circular economy objectives and increasing the sustainability of all metallurgical processing.

Figure 1. Conceptual illustration of red mud valorization within a circular economy, highlighting its conversion into valuable products and metals (Fe, Al, Ti, REEs) to support sustainable resource utilization (Swain, Akcil, and Lee 2022).

1.4.3 Technological Advances Enabling RM Valorisation

Recent advancements in extraction technology have greatly increased the possibilities for the use of RM, which now makes it technologically possible to recover useful elements. Researchers have experimented with several alternative strategies to address the technical problems that arise when working with the complex chemical composition of RM. The various extraction technologies include: hydrometallurgy, pyrometallurgy, magnetic separation, and microwave-assisted. Hydrometallurgical methods are often preferred because they allow extracting the metal(s) of interest by dissolving them in an acidic solution, whereas pyrometallurgical methods involve the transformation of the metal-bearing phases into separate phases during treatment, allowing for easier separation of metals such as iron and titanium. Magnetic separation can also be utilized after thermal or reduction treatment to enhance the recovery of iron-containing phases. One method being particularly investigated is microwave-assisted processing, as it represents a highly effective method for the intensification of extraction technologies. This method provides the opportunity for selective and rapid heating of materials within RM through microwave energy. Rapid heating causes the formation of micro-cracks in the RM, destruction of its structure, and alterations to the phase composition. The altered properties make it possible to increase the ease of transfer of valuable elements from the RM to an aqueous solution, especially those elements trapped within iron oxide or aluminosilicate matrices (Al-Harahsheh and Kingman 2004; Amankwah, Pickles, and Yen 2005; Liu et al. 2020; Singh et al. 2019). Microwave pre-treatment

is therefore becoming increasingly popular as a means of increasing the efficiency of leaching and as a means to increase the total amount of metals recovered from RM.

1.5 Motivation

1.5.1 Need for Sustainable Recovery Routes from Red Mud

Primary ore extraction of value-added metals using the traditional multi-step process includes energy-intensive treatment methods such as beneficiation, high-temperature treatments, and chemical separation. Energy-intensive treatment processes produce large amounts of greenhouse gases, have a negative effect on our environment, and rely heavily on raw primary materials that can be economically and politically constrained. As a result of the increasing number of alternative and more environmentally friendly ways of extracting metals from primary resources, there has been a surge of interest in developing alternative and more environmentally conscious approaches to recovering metals from primary resources.

1.5.2 Advantages of Microwave Treatment for Intensification and Cleaner Processing

In recent years, microwave-based processes have been attracting increased interest as a viable method for mineral processing and waste valorization; this is largely attributed to the nature of how heat is generated by microwaves. Conventional forms of heating generate heat through contact or convection/conduction. Microwaves, however, generate heat internally and selectively by inducing electrical dipoles in the molecular structure of materials having suitable dielectric properties (Al-Harahsheh and Kingman 2004). The ability of microwaves to create localized areas of high temperature, thus shortening processing times and improving overall energy efficiency compared to traditional methods, makes them particularly useful (Amankwah, Pickles, and Yen 2005).

Additionally, it is well documented that the interaction between the microwave absorbing phases (such as Fe_2O_3) and non-responsive phases creates thermal stresses within the material. These thermal stresses can lead to crack development and fragmentation of particles, leading to improvements in element liberation. It has been shown previously that the enhancement of the extraction of REEs from RM, which contains valuable elements such as REEs entrapped in complex mineral matrices, using microwave based treatments to structurally modify the matrix also increases the availability of these elements for subsequent leaching (Al-Harahsheh and Kingman 2004; Amankwah, Pickles, and Yen 2005; Liu et al. 2020; Singh et al. 2019). Furthermore, microwave-based treatments can result in phase transformation of the matrix, which

will be beneficial for the extraction process. Overall, the combination of selective heating of microwave-absorbing phases, the disruption of the structural integrity of those phases, and enhanced mass transfer characteristics during microwave-based treatments is a significant advantage in applying microwave pretreatments for enhancing metal recovery from RM.

2 Research Gap

Although there has been a significant amount of study regarding the recovery of precious metals from RM, many studies are concerned with extracting individual elements using traditional leaching methods. Conventional leaching methods often lack selectivity for the desired element(s), require large amounts of reagents, and result in the simultaneous dissolution of major elements such as iron and aluminum; this results in complications for the subsequent processing steps. Additionally, the extraction of REEs from RM also continues to be an issue because they reside in complex mineral phases (such as iron oxides, aluminosilicate, and titanate) that limit access to them through leaching.

More recent research has evaluated microwave-assisted processing as one possible means of improving extraction efficiencies by creating structural modifications in the form of micro-cracks and/or phase transformation. While much of the recent research concerning microwave-assisted processing focused on the overall recovery of metals from RM, little research exists concerning how REEs behave when subjected to microwave treatment. Specifically, very little research has been conducted evaluating how microwave treatment affects the release or leachability of REEs such as Ce, Nd, Sm, and Eu. As a result, a significant gap exists in the application of microwave-assisted processing to improve the selective extraction of REEs from RM under well-defined conditions. Also, few comparative studies exist where microwave-assisted treatment has been compared directly to conventional direct leaching using consistent experimental conditions.

2.1 Problem Statement

RM is an extremely alkaline industrial product that has both environmental implications and economic value through the content of the highly sought-after REEs. The recovery of REEs is severely limited due to their high affinity to complex matrices of minerals, therefore decreasing both the yield and selectivity of extraction when utilizing conventional leach processes. Conventional processes may be very energy-intensive and produce additional wastes. Microwave-assisted processing provides a potential method for increasing the recovery of REEs from RM by promoting the liberation of RM's constituent phases as well as altering its internal microstructure. Unfortunately, the effect of microwave energy on the various phases of RM has

not been thoroughly investigated, thus limiting the ability to optimize the process. For that reason, the principal problem studied in this investigation was to determine how to increase the yield of REEs extracted from red mud using microwave-assisted pretreatment while maximizing the efficiency and selectivity of the process.

2.2 Research Objectives

The main objective of this study is to evaluate the effect of microwave-assisted pretreatment on the extraction of the selected REEs (Ce, Nd, Sm, and Eu) from the Kazakh Red Mud (KRM) sample.

The specific objectives are:

1. Characterize the mineralogical and structural properties of RM before and after microwave treatment.
2. Investigate the influence of microwave pretreatment on microstructure and phase changes.
3. Evaluate the extraction efficiency of selected REEs under different leaching conditions.
4. Compare microwave-assisted leaching with direct leaching in terms of extraction efficiency.

2.3 Research Questions

This study aims to answer the following questions:

• To what extent can RM be used as a secondary source for REEs recovery using a microwave-assisted leaching process?

• How does microwave treatment affect the structure and accessibility of REE-bearing phases?

• Does microwave pretreatment improve leaching efficiency compared to direct leaching?

• Which leaching system provides better extraction efficiency after microwave treatment?

2.4 Hypotheses

1. Microwave pretreatment changes the structure of RM, improving the liberation and leachability of REE-bearing phases.
2. Microwave-assisted leaching results in higher extraction efficiency compared to direct leaching due to improved accessibility.

2.5 Scope and Limitations

This research investigates a laboratory-scale hydrometallurgy process for the recovery of REEs using Microwave-Assisted Pretreatment from RM. Structural Characterization of the RM was evaluated through various analytical methods, including Scanning Electron Microscopy (SEM), X-Ray Diffraction (XRD), and Fourier Transform Infrared Spectroscopy (FT-IR). Laboratory Leach tests were performed to evaluate the extraction performance of selected REEs (Ce, Nd, Sm, and Eu) under controlled conditions.

The primary limitation of this research includes:

• The studies were performed at the laboratory scale and therefore did not reflect pilot or industrial conditions.
• Only specific REEs were analyzed.

• Assessments of economic feasibility or potential for commercial application of the processes studied were not included.

• Major elements co-extraction (Fe, Al, Ti) was not thoroughly investigated within this project.
• Process parameters are not fully optimized, as the study focuses on comparative evaluation rather than optimization.

3 Literature Review

3.1 Red Mud as a Strategic Secondary Resource for Rare Earth Elements

3.1.1 Global Generation, Environmental Context, and Technospheric Significance

Bauxite residue, widely referred to as RM, has changed from a primarily disposal-based liability to an increasingly strategic secondary feedstock, as global inventory levels continue to grow and conceptual frameworks for recovering additional metals from RM become both technologically broader and increasingly integrated (Evans 2016; Ma et al. 2025). As an outcome of Bayer process digestion, RM forms when Al-bearing minerals dissolve into sodium aluminate liquor, leaving behind Ti–Fe–Si-rich minerals, along with other non-dissolvable or "refractory" phases in the solid residue stream (Evans 2016; Wang et al. 2019; Widyaningsih et al. 2025). In practice, dependent upon bauxite composition and operational efficiency of refineries, there can be as much as one to two tonnes of RM produced for each ton of alumina; this translates into annual production totals that exceed ~150 Mt and cumulative stockpiled quantities which presently total tens of billions of tonnes (Evans 2016; Wang et al. 2019; Ma et al. 2025).

Table 1. Annual red mud generation and global stockpiles.

Parameter	Value
Annual red-mud generation (Mt/yr)	140
Global stockpiles (Mt)	4000

In addition to these factors, there are several physical and chemical attributes that make it difficult to store RM and contain it over time; RM is normally very alkaline (usually pH > 12), finely grained, rich in sodium, and mineralogically heterogeneous. These factors, individually and collectively, create significant risks for seepage, dust mobilization, and geotechnical instability in all types of storage locations (Evans 2016; Swain, Akcil, and Lee 2022; Widyaningsih et al. 2025). Therefore, the strategic basis for value creation has shifted toward economic benefits through the sale of reclaimed materials, as well as reducing risks and achieving circular economy objectives. The latter can be viewed through an entirely different lens when considering RM as a technospheric ore, which extracts Fe, Al, Ti, and other important resources through industrial

processes, rather than enriching them via geological processes (Ma et al. 2025; Schingaro et al. 2025). Of specific interest is titanium: while both iron and aluminum dominate the mass of RM, titanium commonly occurs at levels of 2–10 wt% TiO_2, so that the most common problem with titanium in RM is its accessibility within a chemically resistant, physically encasing matrix (Evans 2016; Schingaro et al. 2025).

3.1.2 Chemical Composition and Mineralogical Hosting of Titanium

From a chemical perspective, RM typically consists of roughly 30–60 wt% of Fe_2O_3, and considerable contributions from Al_2O_3 and SiO_2, along with varying amounts of Na_2O and CaO due to input from process inputs and clarification/digestion conditions (Evans 2016; Widyaningsih et al. 2025; Schingaro et al. 2025). Figure 6 illustrates the typical chemical composition of RM and the relative abundance of selected trace and critical metals.

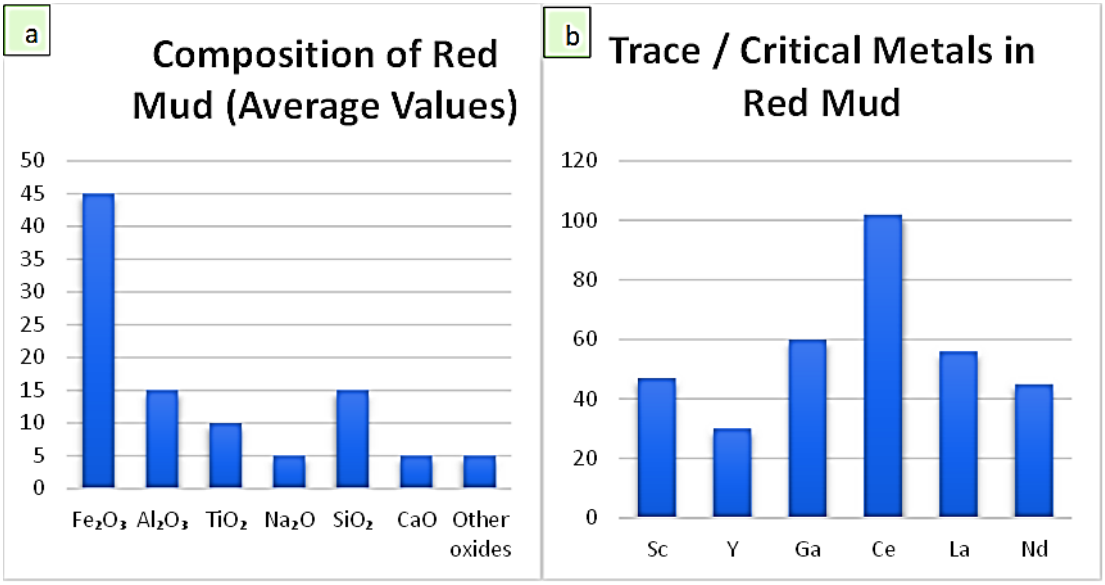

Figure 6. Typical chemical composition of RM and the relative abundance of selected trace and critical metals, (a) average major oxide composition of RM, and (b) concentration of selected REEs.

Titanium is typically found as TiO_2 (primarily anatase and rutile) and sometimes appears as part of complex titanate assemblies or Fe–Ti oxide mixtures, based on the source of the residue and processing conditions (Widyaningsih et al. 2025; Schingaro et al. 2025).

The bulk chemistry of red mud cannot provide much insight into how well various metals will be extracted, since titanium-bearing phases are generally not available as large particles of titanium that are easily dissolved. Titanium is usually found as part of goethite/hematite layers or encapsulated in aluminosilicate matrices and desilication products (DSP's) created during the Bayer process digestion, creating a locked structure that makes it difficult to allow the lixiviants to contact all of the titanium (Widyaningsih et al. 2025; Vind et al. 2018; Schingaro et al. 2025).

Microanalytic research has demonstrated that titanium-containing domains exist at scales below one micron, as part of Fe-rich carriers, as intergrowths that make it impossible for the reaction surfaces to access each other and create a diffusion barrier (Widyaningsih et al. 2025; Vind et al. 2018). Therefore, while the total amount of titanium in the material suggests there could be some value for leachable titanium, the actual leachability is dependent upon the mineralogy of the constituents and their relationship with each other, rather than just the total content. This difference should explain why there were problems observed with direct hydrometallurgy.

Other than the primary components of RM (major oxides), red mud contains trace levels of REEs, including Ce, Nd, Sm, and Eu. These elements have become critical for current technologies, for permanent magnetism, catalysis, and energy storage. While present in very small quantities (typically hundreds to thousands ppm), the quantity of red mud that exists creates a vast potential secondary resource within a circular economy framework.

Significantly, the way in which REEs are associated with minerals in red mud follows an identical pattern to that of titanium. Rather than being contained in distinct mineral phases that are easy to dissolve out, REEs are primarily incorporated into iron oxides, aluminosilicates, and secondary phases created during the Bayer process digestion. This structural relationship limits their availability during hydrometallurgical processing and limits the leaching efficiency under direct leaching conditions. As a result, the recovery of REEs from red mud is controlled by how they are structured in relation to other minerals, not by their concentration. Structural association into mineral phases represents the largest limiting factor for extracting REEs efficiently (Rivera et al. 2018).

As mentioned previously, this structural association not only limits the ease of accessing these elements but also directly controls the effectiveness of hydrometallurgical extraction processes. Due to these similarities in structural association, both titanium and rare earth elements share many common difficulties in terms of extraction. Mineralogic "locking" and phase intergrowth relationships dominate dissolution behaviors far more so than bulk compositions.

While both titanium and REEs are included in discussions about utilizing RM as a value-added material, this study focuses primarily on recovering titanium while using REEs systems to examine differences in structurally controlled extraction behaviors.

In addition to differences in composition, RM possesses physical and chemical attributes (particle size distributions, surface areas, alkalinity, etc.) that affect its reactivity and dissolution behavior. RM typically exhibits fine particle sizes and high surface areas that would seem beneficial for

reactivity; however, these benefits are frequently neutralized through particle aggregation effects that limit access to reactive sites (Wang et al. 2019; Du et al. 2024).

In addition to affecting surface chemistry through alkaline conditions, red mud's high alkalinity (resulting from residual sodium-based compounds from the Bayer process) affects leaching efficiencies. High pH values may cause additional secondary phases to form or inhibit the dissolution of selected elements under specific conditions, thus hindering hydrometallurgical processing (Wang et al. 2019; Zhou et al. 2025).

Therefore, these physical and chemical properties illustrate that not only mineralogical composition is a consideration when assessing the extraction potential of RM, but also surface properties must be taken into account when assessing systems where access to reactive sites and diffusional limitations dominate dissolution behavior.

3.1.3 Microstructural Deportment and Encapsulation Effects

The fundamental metallurgical behavior of RM can be explained through micro-structural deportment, specifically, the location, grain size, internal porosity, and the relationship between titanium-bearing regions and iron-rich regions across different mineralogical investigations (Widyaningsih et al. 2025; Vind et al. 2018; Schingaro et al. 2025).

TiO_2 has been found to occur as small inclusions within hematite, within ferro-titanate type assemblies, or as a component of multi-phase oxides which have developed or altered during digestion and subsequent wash conditioning. These types of associations produce encapsulated phenomena that create diffusive constraints on elemental interactions. The inclusion of titanium-containing domains within ferric oxyhydroxide or aluminosilicate phases creates a physical boundary between the titanium and potential lixiviants, creating slow reaction kinetics even under extremely aggressive conditions (Widyaningsih et al. 2025; Vind et al. 2018).

This provides a rationalization mechanism for the commonly observed large differences between the total mass of titanium present and the degree of extraction achieved, indicating that it is structural entrapment, rather than simply chemical unreactivity, which will typically constitute the greatest barrier. Further, due to variability in the microstructure of RM between sources of bauxite and refining routes (e.g., agglomerative behavior, distribution of amorphous phase material, pore structure), universal leach recipes are generally not transferable without appropriate pre-processing (Widyaningsih et al. 2025; Schingaro et al. 2025).

Consequently, any approach to recovering titanium must take into account both dissolution thermodynamics as well as the microstructural accessibility and transport characteristics

associated with its containment. In general, before undergoing hydrometallurgical processes, RM is washed/dried to remove any remaining soluble alkaline materials and to stabilize the residue prior to downstream processing steps.

These microstructural constraints directly relate to any subsequent hydrometallurgical processes used for recovering structurally bound elements. It is expected that these will exhibit poor extraction efficiencies because of diffusion barriers created by structural boundaries and limited access to reagents. Therefore, conventional direct leaching techniques will likely result in low recoveries of structurally bound elements, whereas pre-treatment techniques capable of altering microstructures may greatly improve extraction efficiencies.

3.2 Hydrometallurgical Pathways for Titanium Recovery

3.2.1 Acid Systems and Selectivity Constraints

Although, hydrometallurgical extraction with mineral-acid systems is currently one of the most studied approaches for processing RM's and, in particular, for dissolution of Ti relevant to associated impurities (Zhou et al. 2025; Ilkhani et al. 2024; Kim, Choi, and Jo 2021), sulphate based systems using sulfuric acid can lead to increased Ti dissolution through the sulfate complexation mechanism; however, this often leads to excessive co-dissolution of iron containing phases which increases the need for additional reagents during processing and causes added complexities for subsequent purification and separation processes (Ilkhani et al. 2024; Kim, Choi, and Jo 2021). In comparison, HCl based systems using chloride complexation can increase oxide solubilization and achieve higher levels of dissolution at optimal temperature and acidity ranges; however, the same issues regarding controlling the amount of impurities taken up into the process streams, in particular Fe and Al, exist at the conditions necessary to break structural lockage (Kim, Choi, and Jo 2021; Zinoveev et al. 2021). Nitric acid systems provide an oxidation component that can potentially impact dissolution kinetics; however, they also introduce potential costs and environmental concerns, particularly when considering handling and treating nitrate post-processing (Ilkhani et al. 2024; Du et al. 2024). Overall, a common trade-off exists across all systems examined to date: those conditions that liberate Ti from structural locks are typically those that will also mobilize significant quantities of Fe and Al, resulting in impurity-rich leach liquors and increasing the burdens of separating these elements (Kim, Choi, and Jo 2021). The structural constraints on selectivity related to recovering Ti from RM are not coincidental or incidental but instead are structurally inherent to the use of chemical aggressiveness as a means of facilitating recovery. Additionally to structural factors, the efficiency of extracting REEs is significantly affected by the choice of acid system. Each acid has different chemical properties in solution that

affect both the mechanisms of dissolution and the complexation of the REEs. HCl has been demonstrated to be particularly useful in terms of rare earth extraction due to its ability to form highly stable chloride complexes that improve solubility and inhibit the precipitation of secondary phases. Chloride-based systems are particularly effective at improving metal extraction due to their ability to form stable metal-chloride complexes and improve the dissolution of structurally locked phase materials (Zinoveev et al. 2021; Li, Eksteen, and Oraby 2019). Sulfuric acid (H_2SO_4), in contrast, may favor the formation of insoluble sulfate compounds, which may restrict the efficiency of extraction regardless of the strength of the acid. Nitric acid (HNO_3) typically demonstrates an intermediate behavior, producing variable extraction efficiencies dependent upon system conditions and mineral composition. As such, differences in acid chemistry directly affect extraction performance when structural accessibilities have been enhanced through pre-treatment. Therefore, the interaction between acid type and mineral structure represents a critical consideration in assessing overall extraction efficiency and should be evaluated when assessing leaching results in complex systems such as RM (Ochsenkühn-Petropulu, Lyberopulu, and Parissakis 1994).

3.2.2 Thermodynamic and Kinetic Controls

The dissolution properties of Ti-bearing phases show both coupled thermodynamics and kinetics (Ilkhani et al. 2024; Du et al. 2024). Anatase and rutile have stable Ti–O bonding networks and a relatively high stability of their lattices. They require sufficient acidity in the system to break down crystal structures and allow Ti into the solution (Ilkhani et al. 2024; Kim, Choi, and Jo 2021). However, it is known that even when all thermodynamic requirements are met, the progression of reactions can be controlled by transport phenomena, especially when there are limited reactive interfaces available due to the encapsulation of reactive solids.

Shrinkage core and mixed reaction-diffusion models were developed specifically for use in solid-oxide systems. These model predictions indicate that diffusion through layer products or the confining matrix can become the limiting factor in controlling the reaction rate (Du et al. 2024). In RM's, where Ti is incorporated into Fe-rich host minerals and/or aluminosilicate frameworks, the amount of diffusion resistance from structural confinement increases. Consequently, the effective leaching rates of materials decrease with increasing acid strength (Widyaningsih et al. 2025; Vind et al. 2018). Additionally, Ti^{4+} hydrolysis behaviors in aqueous solutions can produce polymers or secondary precipitates that will decrease total yield regardless of whether the original compound was dissolved. Overall, these aspects illustrate the limitations to chemically enhancing

dissolution and suggest structural modifications as a necessary condition, not just an optional enhancement, to increase the availability of materials created by micro-cracking.

These issues are most pronounced for rare earth elements, which are usually found embedded in Fe-rich matrices or finely distributed throughout aluminosilicate minerals. Because they are physically contained and are limited in terms of exposure to reactive surfaces, the dissolution of REEs during direct leaching processes is highly dependent upon diffusive kinetics. Therefore, RM, subjected directly to leachants, generally exhibits low extraction efficiencies for REEs; in many cases, below one percent, indicating that leachants cannot effectively reach and dissolve REE-containing phases that are structurally bound together.

The behavior described above has been observed repeatedly in past hydrometallurgical studies, where, although higher concentrations of acids and longer reaction times have been used, the recovery of REEs using direct leaching (DL) continues to be limited. The inefficiency of DL illustrates the need for pre-treatment methods designed to modify the structure of minerals and provide greater access to target elements (Borra et al. 2016).

Two process options will be evaluated within this study: Direct Leaching (DL) and Microwave-Assisted Pretreatment Followed by Leaching (MT + L). Although DL represents traditional hydrometallurgical extraction processes, the MT + L process includes a method to structurally alter mineral samples before subjecting them to leachants in order to improve access to structurally-bound elements.

Aside from diffusion limitations, interactions between leachants and RM matrices also involve surface-passivating effects resulting from secondary-phase formation. During leaching processes, the dissolution of certain components can lead to the re-formation of secondary compounds at particle-surface boundaries, creating passive layers that impede additional mass-transfer and continue to limit overall extraction efficiency (Ilkhani et al. 2024; Du et al. 2024). Secondary-phase formation is particularly problematic in residue systems having significant amounts of iron content, as re-formed Fe-containing phases may inhibit ongoing dissolution of targeted elements.

Additionally, the heterogeneity of RM results in variable rates of dissolution among different phases. Preferential dissolution of certain phases relative to other phases may occur due to differences in solubility or reactivity, resulting in reduced extraction efficiencies even when leachants are highly reactive (Du et al. 2024; Borra et al. 2016). All of these factors illustrate the limitations of using direct-leaching processes and justify developing pre-treatment processes that can physically alter the structure of materials to promote leaching efficiency.

3.2.3 Distribution across geochemical fractions

The majority of the REEs that are found in RM exist within the strongly bound minerals as well as reducible and residue fractions in association with iron oxide matrices and other silicates. The strong bonding of these elements is a major reason why they will remain inaccessible throughout most of the processing steps involved in direct leaching. Because this type of element is so difficult to extract from the red mud matrix, it makes sense that there would be such a low percentage of the REE's being extracted by hydrometallurgical methods (Mittermüller, Saatz, and Daus 2016).

Table 2. Sequential extraction fractions of the REEs and their typical host phases.

Fraction	Extractant	Targeted Binding Form	Typical Host Phases	Typical REE Yield	Leachability
F1 – Easily soluble & ion-exchangeable	0.05 M $Ca(NO_3)_2$	Water-soluble + ion-exchangeable REEs	Surface-adsorbed REEs on clays, carbonates, DSP surfaces	< 1–3 % of total REEs	Very low
F2 – Carbonate-bound & complexed	0.1 M citric acid	Carbonate-associated REEs and weakly complexed REEs	Carbonates, weak surface complexes	10–35 %	Moderate
F3 – Reducible fraction	0.5 M $NH_2OH{\cdot}HCl$ (pH 2)	REEs bound to Fe/Mn oxides	Goethite, hematite, Fe–Mn oxyhydroxides	10–40 %	Moderate–slow
F4 – Acid-soluble fraction	1.4 M HNO_3	Phosphate-bound and refractory REEs	Monazite, xenotime, REE-phosphates, titanates	15–50 %	Slow
Residual fraction	Aqua regia digestion	Structurally bound REEs	Titanates, silicates, refractory oxides	Remaining fraction	Very difficult

3.3 Pretreatment and Phase Engineering Strategies

3.3.1 Thermal and Chemical Reconstruction

Several chemical pretreatments (i.e., thermal roasting, alkali activation, carbothermic reduction, and magnetic separation) have been used to break down the structural constraints of refractory materials (RM), in order to create new solid-phase structures for extraction by leaching (Schingaro et al. 2025; Li et al. 2023; Cozzolino 2023; Loginova and Kyrchikov 2021). Alkaline roasting at high temperatures is able to transform non-soluble aluminosilicate compounds into soluble sodium-aluminate compounds as well as modify Ti associations according to the reaction conditions (temperature, leaching time, ratio of reagents) (Li et al. 2023; Cozzolino 2023).

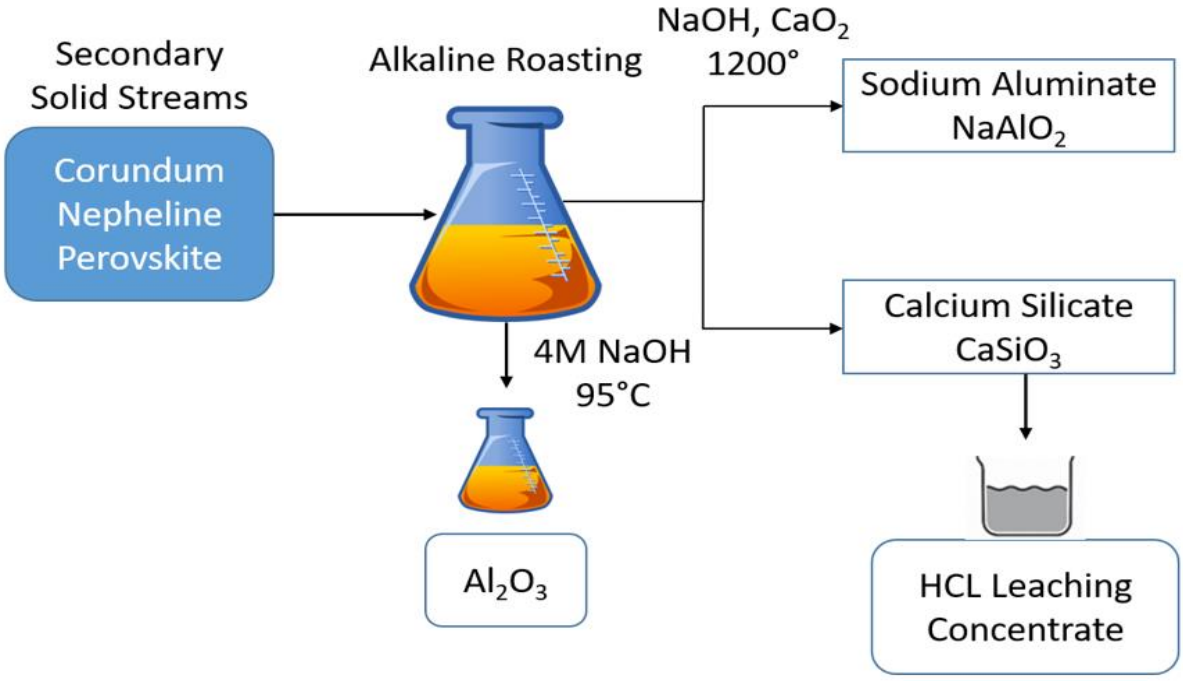

Figure 7. Schematic representation of alkaline roasting and subsequent leaching pathways for metal recovery from RM.

The combination of carbothermic reduction and magnetic separation is able to promote phase transformations of iron and physically separate it from other phases, thus creating indirect access to Ti-rich domains (Liu et al. 2020; Loginova and Kyrchikov 2021). However, most of the above treatments require high amounts of energy as well as long processing times and are generally composed of multiple steps. Furthermore, over-processing may result in loss of Ti during subsequent metallurgical processes. For this reason, attention has recently turned to strategies aimed at reducing processing times through either mechanical or heat-intensive processes, which

would allow rapid structural breakdown and increased surface area within refractory materials without prolonged exposure to high temperatures.

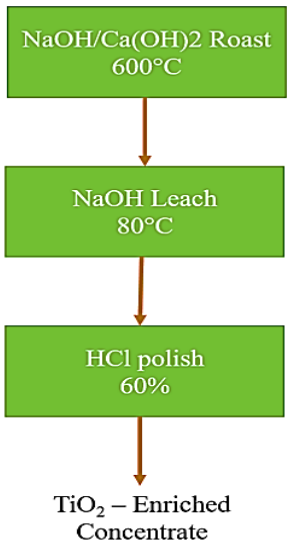

Figure 8. Simplified process flow for NaOH/$Ca(OH)_2$ roasting, alkaline leaching, and acid polishing for TiO_2-enriched concentrate production.

3.3.2 Microwave-Assisted Structural Intensification

Microwave (MW) treatment represents an alternative mechanism of heat application compared to traditional conductive methods; microwave energy is absorbed within the dielectric properties of materials throughout the volume of the material as opposed to at its surface. Dielectric absorption causes specific phases to selectively absorb microwave energy. Therefore, when applied to multiphase reactive metal matrices, this energy creates localized areas of elevated temperatures and internal thermal gradients. As these gradients exist across differing thermally expansive phases, they create stresses at interfaces between them. When these stresses become great enough, cracks form at these locations. Crack growth also initiates grain boundary separation and defects that ultimately lead to disruptions in the microstructure. Such disruptions provide enhanced pore space and reduced diffusion barrier resistance to subsequent leachants (Liu et al. 2020; Singh et al. 2019).

Importantly, microwave-assisted intensification does not require the complete transformation of phases to achieve desired effects. Phase weakening through localized damage can facilitate increased diffusion access and leaching rates even in highly diffusion-limited systems (Liu et al. 2020; Singh et al. 2019; Du et al. 2024). For example, studies involving microwave-driven transformation of hematite into magnetite in controlled environments demonstrate targeted phase transformation capabilities. While many titanium-based processes focus upon enhancing diffusion access over achieving total Fe phase transformation (Swain, Akcil, and Lee 2022; Schingaro et al.

2025); similar examples of microwave-assisted pretreatment to improve the extraction of REEs from RM show potential for increasing diffusion access through thermal-induced cracking and structural degradation.

As related to the extraction of REEs from RM, microwave-assisted pretreatment has been examined extensively for the enhancement of leaching efficiencies. Rapid heating of dielectric mineral phases in the presence of microwave radiation generates internal thermal gradients, resulting in the rapid formation of micro-cracks. Micro-crack formation results in an increase in porosity and enhances the penetration depth of leaching agents. Increased porosity reduces diffusion barriers and improves reaction kinetics.

For the purpose of extracting REEs, microwave-assisted pre-treatment plays a major role in releasing elements that are physically or chemically attached to the residue matrix by altering the physical and chemical characteristics of the residue matrix. Several studies have shown that the use of microwave-assisted systems provides significant increases in REE recovery when compared to direct leaching. Microwave heating has provided a means for coupling thermal and chemical pathways to enable specific liberation of elements. This enhancement is particularly relevant in diffusion-limited systems where accessibility is a limiting step prior to chemical reactivity (Li, Eksteen, and Oraby 2019).

3.3.3 Dielectric Selectivity and Phase-Specific Heating

The effectiveness of MW is dependent upon the distribution of both dielectric constant and loss factor in different phases within a material (Al-Harahsheh and Kingman 2004; Amankwah, Pickles, and Yen 2005). Typically, iron oxides are coupled much better to microwaves than silica-rich or aluminosilicates; this allows for selective heating, which will preferentially weaken (disrupt) encapsulating Fe-bearing matrices while maintaining (preserving) Ti-bearing areas (Amankwah, Pickles, and Yen 2005; Chen et al. 2016). Preferential heating creates internal stresses, and differential heating leads to increased internal stress gradients that enhance fracture development and increase surface area available for mass transport during leaching (Liu et al. 2020; Singh et al. 2019).

Mechanistically, there is also a need to understand how to scale up from laboratory tests to operational reactors, specifically, understanding of penetration depth into a material, whether a microwave field can be made as uniform throughout a reaction vessel, and finally, designing a reactor such that it maximizes exposure of the material to the microwave energy source, all of these need to be considered when the materials being treated have heterogeneous dielectrics that may lead to uneven heating at larger scales (Al-Harahsheh and Kingman 2004; Amankwah,

Pickles, and Yen 2005). Therefore, mechanistic testing should combine microwave treatment with structural analysis and kinetic modeling rather than solely using recovery metrics.

3.4 Structural Characterization Framework

To study the MW-assisted recovery of Ti from RM, an integral structural study is necessary. Using XRD, which permits an observation of the progression of the formation of crystalline phases and the degree of broadening of peaks, which indicates the presence of defects or a partial conversion (Schiningo et al., 2025; Widyaningsih et al., 2025). Moreover, the use of FTIR provides further information related to the transformation of titanium-oxygen and iron-oxygen bond environments, as well as the behavior of hydroxyl groups (Supriadi et al., 2025). SEM-EDS also gives evidence of morphological transformations in terms of crack propagation, surface roughness, and intergranular separation (Vind et al., 2018; Widyaningsih et al., 2025). Most importantly, it is essential to show that the structural modifications observed through various analytical techniques have a relationship with the extraction efficiency and that higher levels of titanium recovery result from a reduction in diffusion resistances and an increased accessibility to titanium, as opposed to only a greater solubilization of ferric oxide.

The use of these analytical techniques together creates a basis for comparison of structural modifications produced by microwave treatment to variations in leaching extraction performance. The association among multiple characterization techniques is even more critical for materials such as red mud that contain numerous chemical components. For example, while X-ray Fluorescence (XRF) can provide quantitative data concerning the total elemental content of a sample, it cannot provide information about how the individual elements are dispersed throughout different mineral phases. In addition, XRD can identify crystalline phases; however, amorphous or poorly crystallized phases may be difficult to detect via XRD, but may still have a considerable influence on leaching performance (Du et al., 2024; Schingingo et al., 2025). Also, SEM-EDS provides the capability to view microstructural features, including particle shape, particle aggregation, and micro-cracking, all of which relate to the effects of leaching on the material's accessibility and transport properties (Schingaro et al., 2025; Vind et al., 2018). Lastly, FTIR contributes by providing information relating to the types of bond environments and functional groups contained within a sample before leaching occurs and thus could reflect modifications occurring during pre-treatment (Supriadi et al., 2025). Therefore, it is evident that an application involving multiple analytical techniques will be needed to attain a comprehensive understanding of both the chemistry and structure of the sample to allow for more reasonable interpretation of leaching performance and process efficiencies.

3.5 Integrated Perspective on Microwave-Enhanced Recovery from Red Mud

A common trend exists in the literature about RM as a significant source of Ti: it has been found that Ti is almost always chemically bound within iron-rich or aluminosilicate matrices, which results in its continued leaching being limited by diffusion barriers and selectivity (Widyaningsih et al. 2025; Vind et al. 2018; Schingaro et al. 2025). Acidic dissolution of Ti is possible at high concentrations of acidity; however, these acidic conditions often result in the release of large quantities of both aluminum and iron into solution, thereby creating additional problems downstream and limiting selectivity (Ilkhani et al. 2024; Kim, Choi, and Jo 2021).

Therefore, for Ti-based recovery from RM, pretreatment methods are needed to provide pathways for preferential disruption of encapsulating matrix materials. Microwave (MW) assisted processing represents one method to achieve increased rates of reaction through localized heat generation (dielectric heating), localized mechanical damage due to thermal expansion-induced stresses, and localized alteration of structure that can lead to increased permeability and improved access to leachants (Al-Harahsheh and Kingman 2004; Liu et al. 2020; Singh et al. 2019). When used in conjunction with hydrometallurgical processes that have some degree of control over chemistry, along with validation using integrated analytical techniques (e.g., XRF, XRD, FTIR, SEM-EDS), it appears possible to use microwave pre treatment to increase the accessibility of Ti while reducing the required concentration of reagents needed for leaching and reducing secondary wastes, which would be in alignment with larger circular economy goals (Ma et al. 2025).

3.5.1 Process Intensification Logic within Titanium-Focused Valorization

Recovery of titanium via the valorization of RM residues is contingent upon the acceptance that the extraction of Ti is seldom the primary objective of an extraction process, however, when multi-metal recovery processes are employed for the sequential or selective extraction of metals such as Ti, Fe, Al, Na, and potentially REE's based on the chemical composition of the residues, these metal recoveries are performed through sequential or selective dissolution and separation strategies (Ma et al. 2025; Schingaro et al. 2025; Kim, Choi, and Jo 2021). These combined extraction strategies require that pretreatment methods used to release metals into solutions not only provide "increased dissolution" but also preserve Ti-bearing minerals while increasing the accessibility of surrounding mineral matrices, a critical distinction that separates Ti-centric extraction strategies from those that have been optimized for Fe upgrading or Sc selectivity.

The intensification strategy followed directly from the microstructural constraints previously discussed. Encapsulation creates diffusion-limited dissolution; therefore, aggressive chemistry

alone will create increased impurities dissolved. Therefore, structural modifications before leaching become the key factor for creating conditions for enhanced dissolution. Microwave (MW) treatment serves as a conditioning step for changing the physical constraints controlling dissolution rates rather than providing a replacement for hydrometallurgical treatments (Al-Harahsheh and Kingman 2004; Liu et al. 2020; Singh et al. 2019). Studies of multiple stages of RM processing have demonstrated time after time that the structural conditioning of the initial matrices determines the subsequent selectivity windows for extracting various metals (Zhou et al. 2025; Ilkhani et al. 2024; Kim, Choi, and Jo 2021). When Fe is rapidly extracted and controls solution chemistry, then Ti recovery is masked by impurity loadings; when Fe-rich matrices are structurally broken down with minimal chemical dissolution, then Ti accessibility may increase without corresponding increases in impurities, an additional justification for the strategic use of controlled dielectric intensified treatments.

Although this conceptual structure was initially established for titanium-containing systems, similar structural and kinetic constraints exist for other rare earth elements (REE) in red mud. The extraction of elements such as cerium (Ce), neodymium (Nd), samarium (Sm), and europium (Eu) is generally more difficult due to their higher degree of dispersion and lower concentration levels than titanium, and thus, is subject to greater sensitivity to microstructural accessibility and diffusion limitations. Thus, as with all RM contained REE's, microwave-assisted pretreatment should produce particularly favorable results, as improved permeability and phase exposure during microwave-assisted pretreatment can lead to significant enhancements in leachability compared to direct leach systems.

3.5.2 Comparative Assessment of Microwave versus Conventional Heating

Thermal treatment using a traditional approach relies upon conduction heat transfer and extended holding times for temperature distribution throughout a sample; while this method is capable of transforming phase structure, it generally cannot selectively target grain boundaries. On the other hand, MW radiation allows for volumetric heating of materials through dielectrically coupled absorption of microwave energy, resulting in internal temperature gradient formation and localized stresses developed as a result of non-uniform heating across different regions of solid samples (Al-Harahsheh and Kingman 2004; Amankwah, Pickles, and Yen 2005; Chen et al. 2016). In iron-rich systems, comparative studies show that under specific conditions, MW roasting can enhance transformation rates and lower energy consumption compared to roasting using conventional methods (Swain, Akcil, and Lee 2022; Schingaro et al. 2025).

The relevance of MW processing in enhancing titanium accessibility is less about achieving full transformation and more about creating internal stresses and micro-fractures in a sample without subjecting it to long-term high-temperature exposures. This consideration is especially important due to potential drawbacks associated with sintering, pore collapse, and density increases when a sample is subjected to very large or extreme roasting temperatures. However, there are several issues related to MW processing that require careful consideration, including limited penetration depths of MW fields, varying levels of field uniformity over larger spatial areas, and varying degrees of dielectric heterogeneity that could create hot spots and/or poorly heated regions during MW processing (Al-Harahsheh and Kingman 2004; Amankwah, Pickles, and Yen 2005). Therefore, further mechanistic validation of MW processing via structural characterization and kinetic analysis is required.

3.5.3 Structural Evolution and Leaching Performance Correlation

The consensus among researchers has been that structural analysis should be done prior to making a claim about how material properties may have been altered due to MW processing. Structural modifications and the occurrence of phase transformations are demonstrated by XRD peak broadening and intensity shifting (Widyaningsih et al. 2025; Schingaro et al. 2025), changes in bond environment related to Ti–O and Fe–O structures are indicated by variations in FTIR bands (Supriadi et al. 2025); crack propagation and porosity development as a result of degradation of the matrix material are directly observed through SEM-EDS imaging (Widyaningsih et al. 2025; Vind et al. 2018).

It is important to distinguish between simply documenting change and demonstrating a relationship. For Ti-based systems, it will be required to demonstrate that an increase in recovery is due to an improvement in access to the internal structure, as opposed to some arbitrary dissolution of the surrounding matrix material, specifically when the primary contributor to leaching chemistry is the dissolution of iron. As previously stated for diffusion-limited matrices, small increases in permeability can significantly affect the kinetics (Du et al. 2024). Thus, MW-assisted recovery of Ti requires integration of both structural indicators and kinetic models with solution chemistry to avoid attributing recovery improvements entirely to dielectric effects.

3.5.4 Kinetic Regime Shifts under Structural Modification

The rate-limiting step in shrinkage-controlled dissolution processes, such as those occurring in encapsulated titanium (Ti) domains contained within iron-rich (Fe) matrices, will vary with respect to either surface reaction control or diffusion control as dictated by structural accessibility (Du et

al. 2024). Typically, due to structural barriers (i.e., acid penetration), the encapsulation of Ti domains within Fe-rich matrices limits the extent of acid penetration into these regions, resulting in diffusion limitation (Widyaningsih et al. 2025; Vind et al. 2018). However, MW induced weakening of the structure will result in a reduction in the length of the diffusion path through the material, an increase in the amount of pore space available within the material, and provide access to previously inaccessible areas of the Ti surface; all of which contribute to a transition from diffusion limited to mixed controlled regimes, while also causing an apparent increase in the extraction rate without corresponding increases in either acid concentration or temperature.

In terms of economics, the transition described above has significant implications as it represents a means to potentially reduce the quantity of reagents consumed during processing, along with reducing energy requirements (Ilkhani et al. 2024; Kim, Choi, and Jo 2021) and supporting sustainable development goals related to minimizing environmental impact and maximizing recycling of materials (Ma et al. 2025).

3.5.5 Titanium Preservation and Impurity Management

A major difficulty in recovering Ti from RM is finding a way to maintain Ti structure while minimizing Fe co-dissolution. An overabundance of dissolved Fe creates an impurity burden on the system and changes the chemistry of the solution in such a manner as to create additional challenges for future separations and possibly to destabilize Ti-based association groups (Kim, Choi, and Jo 2021). Selective degradation of encapsulating matrices using MW could provide a method to separate access and aggressive chemistry in order to enhance the accessibility of Ti while minimizing the mobilization of impurities.

It is especially important to preserve this selectivity in those applications where Ti recovery has to occur simultaneously with sequential separation of Fe and Al (or other associated elements) or co-products. Therefore, Ti-focused intensified process development should be viewed through the lens of multi-element RM processing processes and their integrated literature (Ma et al. 2025; Kim, Choi, and Jo 2021).

3.5.6 Broader Context within Circular Economy and Secondary Resource Utilization

The transformation of RM into an ore of the technosphere is consistent with larger changes in resource management where industrial wastes are viewed as secondary feedstocks rather than inert waste (Ma et al. 2025; Schingaro et al. 2025). Since titanium has a high value due to the wide use for pigments, alloys and other advanced materials, it can be seen as one of the most promising

resources to be recovered from RM; yet, for this to occur sustainably, we need to find a balance between how much of the material can be recovered and the amount of chemicals needed to recover them (reagent intensity), the amount of energy used to recover the material and generate additional wastes. Therefore, methods that improve access to the material but do so under less severe chemical conditions are closer aligned to current paradigms for resource efficiency (Al-Harahsheh and Kingman 2004; Ma et al. 2025). Pretreating RM using MW treatment and integrating it with controlled leach times provides a means to better match these paradigms by removing diffusion barriers and increasing the rate of reaction for RM without needing to apply extreme process conditions.

3.6 Synthesis and Positioning for Microwave-Assisted Recovery from Red Mud

Collectively, the data from the articles discussed above support three related propositions. Firstly, RM has substantial deposits of titanium and REEs. These two elements are typically held in solid solution form, primarily within iron-rich and aluminosilicate matrices (Wang et al. 2019; Schingaro et al. 2025; Du et al. 2024; Rivera et al. 2018). Secondly, direct hydrometallurgy has several kinetic and selectivity barriers caused by diffusion and impurities being transported during co-dissolution (Ilkhani et al. 2024; Du et al. 2024; Kim, Choi, and Jo 2021; Borra et al. 2016). Although direct leaching is commonly used because it is simple to operate and compatible with conventional hydrometallurgical operations, its success depends largely on the complexity of the minerals present. For example, many of the REEs contained in RM are chemically bonded within stable phases (Borra et al. 2016; Li, Eksteen, and Oraby 2019) and therefore require considerable leaching time for removal. Thirdly, there is widespread recognition that the primary limitation to efficiently recovering titanium is not chemical stability but structural encapsulation (Vind et al. 2018). Therefore, one of the most critical challenges associated with improving extraction efficiency is reducing or eliminating the effects of structural encapsulation. Various pre-treatment approaches have been suggested for achieving this goal, including microwave activation, thermal treatment, and chemical conditioning in order to alter the mineral structure, increase phase release, and increase leach efficiency (Du et al. 2024; Borra et al. 2016). Dissolving rare earth oxides using HCl can be described by Equation 1:

$$REE_2O_3 + 6HCl \rightarrow 2REE^{3+} + 6Cl^- + 3H_2O \qquad (1)$$

Therefore, within this context, various pre-treatment methods designed to modify the structure of the mineral are essential. Traditional thermal and chemical reconstructive processes may provide improved extraction results but usually involve higher energy inputs and increased process integration complexity (Li et al. 2023; Cozzolino 2023; Loginova and Kyrchikov 2021).

Microwave-assisted processing offers an alternative route to achieve process intensification through selective dielectric heating of materials, localized mechanical stresses developed during rapid heating, and microstructural damage (Al-Harahsheh and Kingman 2004; Liu et al. 2020; Singh et al. 2019). The use of advanced analytical techniques (XRF, XRD, FTIR, SEM-EDS) will allow researchers to develop correlations between phase transformations in the mineral and leaching performance. Furthermore, these analytical techniques will enable researchers to determine if the observed increases in extraction rates are due to enhanced structural accessibility or general matrix dissolution (Widyaningsih et al. 2025; Supriadi et al. 2025). Therefore, microwave-assisted acid leaching represents an additional conceptually based step beyond traditional RM valorization studies focused on microstructure-related obstacles to elemental accessibility prior to chemical extraction, while also allowing researchers to minimize the amount of reagents consumed during the process. In this paper, we demonstrate how this methodology is being applied to Kazakh red mud (KRM) to assess microwave-based structural modifications prior to subsequent acid leaching.

This work compares extraction efficiencies for selected metals obtained by applying direct leaching (DL) versus microwave-assisted leaching (MT+qewfe\rzgL) conditions. We particularly focus on determining whether increased extraction efficiencies are achieved due to enhanced structural accessibility or alterations in bulk composition. Therefore, our comprehensive approach allows us to directly relate microstructural transformation with extraction behavior.

4 Materials and Methods

The kiln-treated Kazakh Red Mud (KRM) sample was collected from the Pavlodar Aluminum Plant (PAZ), Pavlodar, Kazakhstan, and represents RM that underwent controlled thermal treatment under industrially relevant kiln conditions. All the reagents used in this study were of analytical grade and were used without further purification.

The methodological approach of this research experiment was designed to investigate how the application of microwave-assisted pretreatment can be utilized to alter the extraction behaviors of a number of the selected REEs (Ce, Nd, Sm, and Eu) that occur in the form of rare earth minerals or compounds in Kazakh Red Mud (KRM). An additional objective was to find a correlation between the structural modifications created due to microwave treatment of KRM samples and their corresponding leaching performances when subjected to three different acidic systems. In order to achieve these objectives, an overall sequential methodology was developed, which included four major stages:

Stage i. Sample preparation and homogenization.

During Stage i, a number of large-sized KRM sample was crushed into smaller particles through various mechanical means (such as crushing and milling). The milled materials were then passed through a series of sieves in order to create a uniform powdered sample. Homogenizing the powder is essential for the establishment of reliable results because it minimizes the effects caused by variations in particle sizes on the subsequent process steps (extraction and analysis). Stage ii. Microwave-assisted pretreatment.

Microwave-assisted pretreatment was employed as a method to create microstructural modifications within the material. For this portion of the study, microwave energy was directed at the KRM sample utilizing a constant power setting of 1500 watts for a time interval of sixty minutes. As previously mentioned, microwave treatment induces selective heating of the heterogeneous mineral matrix present in red mud. Therefore, microwave treatment produces microstructural transformations, including internal stresses within the individual grains of red mud and/or localized micro-cracking and/or localized phase transformation. It is anticipated that these microstructural transformations will allow greater access to REE-containing phases present in the RM and thus enhance leaching.

Stages iii and iv. Acid leaching and Physicochemical Characterization/Analysis. Both untreated (raw KRM) and microwave-treated (MT) samples underwent acid leaching using three different mineral acids, H_2SO_4 (sulfuric acid), HCl (hydrochloric acid), and HNO_3 (nitric acid). Stages iii and iv were conducted so as to evaluate the relative extraction efficiencies of the selected REEs present in the RM when using different lixiviant systems, assess whether the microwave pretreatment enhanced the extraction performance, and ultimately provide information about the physical and chemical characteristics associated with the treated versus untreated samples.

The final stage consisted of analyzing both treated and untreated KRM samples employing multiple analytical methods. The primary methods involved in phase identification were X-ray Diffraction (XRD) and Microstructural and Elemental Analysis via Scanning Electron Microscopy coupled with Energy Dispersive Spectroscopy (SEM-EDS). Additional structural analyses were performed via Fourier Transform InfraRed Spectroscopy (FTIR). Finally, chemical analysis via X-Ray Fluorescence (XRF) was used to determine the bulk chemical compositions of both the raw KRM samples and the leached residues. Additionally, Inductively Coupled Plasma Optical Emission Spectrometry (ICP-OES) was employed to analyze the elemental concentrations in each leachate.

4.1 Sample preparation process

4.1.1 Jaw Crusher

RM samples underwent a systematic reduction of their particle size through a comminution procedure to allow them to be tested and analyzed properly. Three consecutive steps involving the reduction of particle size and the improvement of homogeneity in the materials were used to prepare the samples. First, initial sample reductions were completed by reducing bulk samples of RM to coarse particulate material using a jaw crusher, as depicted in Figure 9. A mechanical advantage was achieved when a stationary jaw crushed the larger red mud agglomerates against a moving jaw as it oscillated back and forth. The jaw-crushing provided the primary stage of processing, which allowed for a consistent and controlled feed size to be provided to the next processing stage.

Figure 9. Jaw crusher used for comminution of KRM sample.

4.1.2 Drum Mill

Intermediate grinding of the crushed particles took place using a drum mill (see Figure 10). The rotational action of the drum caused constant grinding as well as mixing; this process resulted in additional size reduction while also increasing the homogeneity of the crushed particles. The purpose of the intermediate grinding process was to achieve an increase in the uniformity of the particle size distribution before the final milling process.

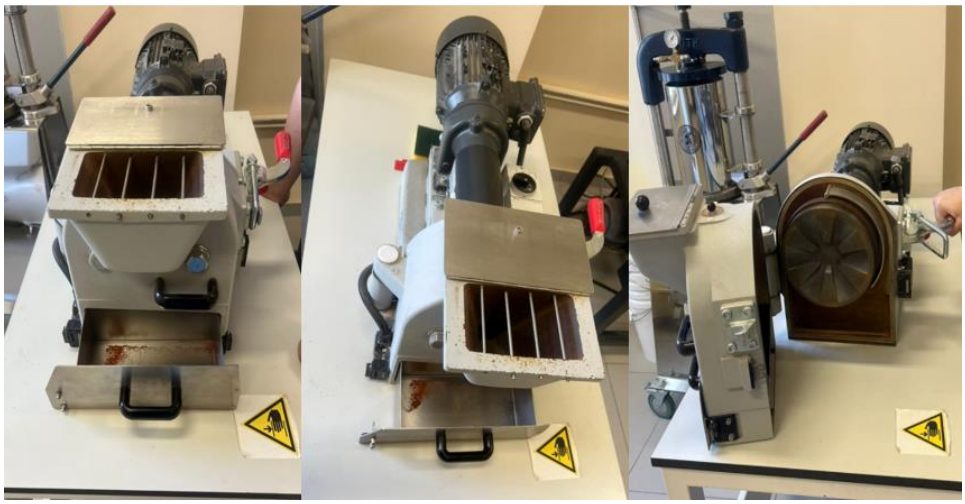

Figure 10. Drum mill

4.1.3 Ball milling

The processed material was then subjected to a ball milling process (Figure 11), where it was ground into an extremely fine and homogeneous powder. Ball milling is a size reduction method that involves grinding media repeatedly colliding with powder particles during the process of producing a powder. Therefore, there are several important variables that need to be monitored in order to achieve efficient grinding without excessive heat generation or degradation of the properties of the powder being milled.

Figure 11. Ball mill

4.1.4 Powdered KRM sample

After complete milling and grinding, the powdered KRM sample was put into airtight containers to protect the sample from contamination or moisture, as shown in Figure 12. As a result of this process, the final samples produced by milling displayed improved uniformity in their particle sizes, thus providing a means to analyze these samples further through additional physicochemical and structural testing.

Figure 12. Powdered KRM sample after grinding and sieving, showing uniform particle size.

4.2 Experimental Objective

The microwave-assisted pretreatment process was used to modify the physical and chemical characteristics of the KRM sample and to increase the degree of availability of phases containing REEs. MW Pretreatment was employed using a lab-scale microwave muffle oven with an operational frequency of 2.45GHz, and operational power level of 1,500 W. While microwave-based treatments may be affected by the amount of time subjected to radiation, sample weight, particle size, and operation conditions (e.g., moisture), the KRM samples treated here were exposed to a consistent set of conditions: 1,500W for 60 minutes. Microwave radiation produces selective heating effects on the complex mineral matrix present in RM, where particles having higher dielectric losses (such as those containing iron-like hematite and magnetite, as well as titanium-bearing phases) will heat volumetrically at rates faster than other particles in the sample. Other particles or phases that have lower absorption capability will exhibit slower volumetric heating. Differences in volumetric heating rates can produce differences in the rate at which each type of particle is heated, creating temperature gradients both internally and between different types of minerals. As a result of these temperature gradients, thermal stresses develop in the RM, producing micro-cracks in the minerals, fracturing them into smaller fragments, and converting some of the original minerals from one form to another. These structural modifications make it easier to access REE-containing phases that are generally confined in iron-rich and aluminosilicate matrices. Following MW pretreatment, the samples were cooled back to ambient temperature and placed in airtight containers to prevent contamination.

The total microwave energy input (E) is defined as:

$$E=P\times t \qquad (2)$$

where

E = total absorbed energy (J)

P = microwave power (W, fixed)

t = exposure time (s)

4.2.1 Microwave Treatment System Description

Microwave pretreatment trials were conducted using an advanced microwave muffle oven PYRO 064 Advanced Microwave Muffle Furnace (see Fig. 13), which is set at a fixed frequency of 2.45 GHz. This unit includes a closed cavity with high-temperature insulating lining, which allows for the rapid volume heating of materials with a high dielectric loss property. Trials with microwave processing were run under conditions of constant power of 1500W and time of 60 min. Samples used in these trials were placed inside a microwave-transparent ceramic crucible contained within the processing chamber of the microwave processing system. Heating in this system occurs through a dielectric process by means of the interaction between the electromagnetic field and the mineral phase(s) found in the matrix of the red mud sample. Hematite, magnetite, and other iron-bearing minerals, along with titaniferous minerals, have higher efficiency in absorbing microwave energy than do mineral phases with low dielectric loss factor; thus, they are heated rapidly, while those with lower absorption capacity heat much more slowly. The difference in absorption rate creates internal temperature gradient differences throughout the sample.

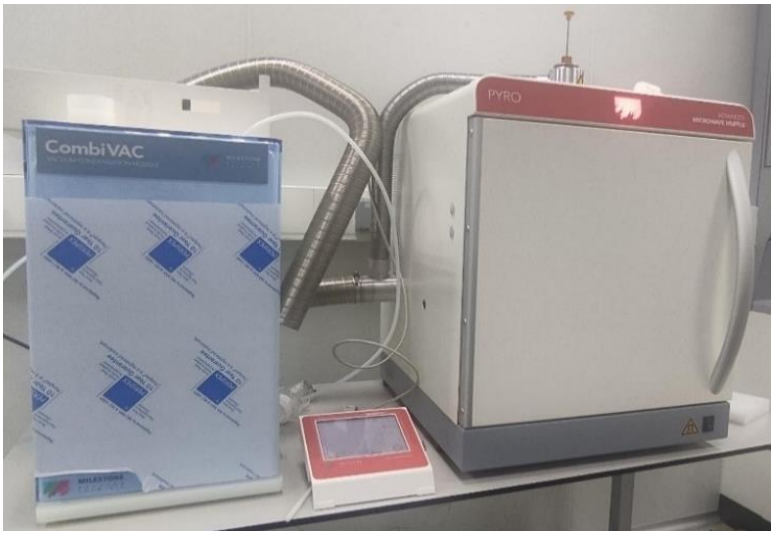

Figure 13. Advanced microwave muffle furnace (064 PYRO) used for microwave-assisted pretreatment of KRM samples.

Prior to microwave pretreatment, RM samples were washed with de-ionised water to remove alkaline-soluble phases that are associated with the Bayer process. Three cycles of washing were carried out using a solid to liquid ratio of 1:10 w/v at 300 rpm for thirty minutes per cycle. Each cycle was followed by vacuum filtration and centrifugation in order to ensure the complete

removal of fine particles from the sample. The washed material was then dried at 105° c for twenty-four hours. The pretreatment step reduced the influence of sodium compounds left over from the Bayer process on acid consumption and improved leach selectivity.

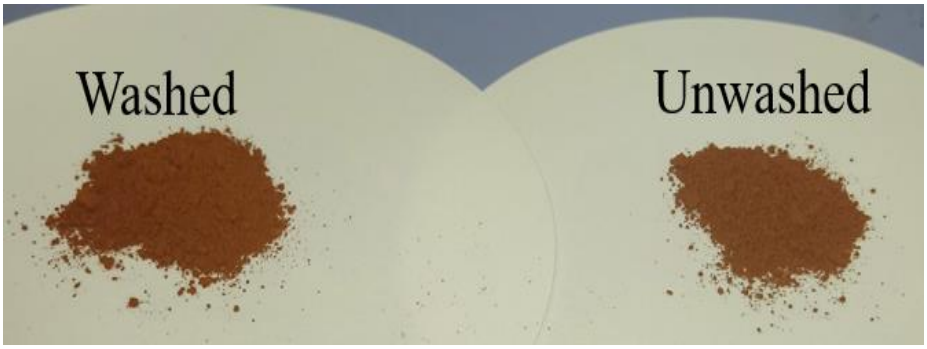

Figure 14. Comparison of washed and unwashed red mud samples after drying at 105 °C.

Table 3. Washing conditions used for KRM samples before microwave pretreatment.

Parameter	Value
Washing medium	Deionized water
Solid/liquid ratio	1:10 (w/v)
Temperature	20–25 °C
Stirring speed	300 rpm
Washing time	30 min per cycle
Number of cycles	3
Separation	Vacuum filtration / centrifugation
Drying	105 °C for 24 h

4.3 Leaching Experiments and Experimental Design

Following the washing pretreatment, leaching experiments were conducted using three mineral acids: sulfuric acid (H_2SO_4), nitric acid (HNO_3), and hydrochloric acid (HCl).

Figure 15. Reagents used in leaching experiments: sulfuric acid (H_2SO_4), nitric acid (HNO_3), and hydrochloric acid (HCl).

The concentration of acids has been set at 3.0 M for H_2SO_4; 6.0 M for HNO_3, and 1.5 M for HCl. Also the same solid-to-liquid ratio was used during the experiments with 2.5 % (w/v) for sulfuric acid and 5 % (w/v) for nitric and hydrochloric acid systems. All experiments have been performed in a 250 mL reactor with a constant temperature of 90 °C and a leaching period of 60 minutes under continuous stirring. There are two methods of treatment employed during this work: Direct Leaching (DL); and Microwave Assisted Leaching (MT+L). During the DL method, the washed samples were used directly for acid leaching without preliminary microwave heating. An effective leaching time that is used for comparison was 60 min. for all acid systems. During the MT + L method, the samples were preliminarily heated by microwave radiation at a constant power of 1500 W and then subjected to the above-mentioned acid leaching conditions. Microwave radiation was applied before the traditional leaching procedure to cause structural changes in the RM matrix. Three experiments represent each processing route that corresponds to three types of acids (H_2SO_4, HNO_3, and HCl). Therefore, it is possible to compare DL and MT + L processes with equal parameters, i.e. to evaluate the impact of microwave heating on the extraction efficiency of the selected REEs (Nd, Ce, Sm, Eu).

Table 4. Direct leaching (DL) conditions for selected experiments.

Test code	Acid	Process	Microwave	Time (min)	Solid weight (g)
KRM–SA–DL–60	H_2SO_4	DL	No	60	6.25
KRM–NA–DL–60	HNO_3	DL	No	60	12.5
KRM–HA–DL–60	HCl	DL	No	60	12.5

Table 5. Microwave-assisted leaching (MT+L) conditions for selected experiments.

Test code	Acid	Process	Microwave	Power (W)	Time (min)	Solid weight (g)
KRM–SA–MT–1500–60	H_2SO_4	MT+L	Yes	1500	60	6.25
KRM–NA–MT–1500–60	HNO_3	MT+L	Yes	1500	60	12.5
KRM–HA–MT–1500–60	HCl	MT+L	Yes	1500	60	12.5

4.4 Characterization Techniques

4.4.1 SEM–EDS Characterization

The use of the field emission dual beam SEM-EDS system (Carl Zeiss CrossBeam 540) allowed for detailed, high-resolution microstructural and elemental examinations of RM samples before and after microwave treatment. The CrossBeam system uses a Gemini field emission SEM column that can be coupled with a focused ion beam (FIB). This allows for selective milling and unmasking of buried structures as needed. Secondary electron (SE) and backscatter electron (BSE) imaging studies were conducted to determine surface morphology and composition contrasts at the sample's surfaces. Energy dispersive X-ray spectroscopy (EDS) was used to perform qualitative and semi-quantitative microchemical mappings of Fe oxide, aluminosilicate, titanate, and trace REEs bearing phases. The CrossBeam system was run in the ZEN software environment, which provides an interface to perform fully automatic navigation of stages and pattern-based imaging. These capabilities allow researchers to analyze multiple sites at different magnifications in heterogeneous red mud samples. The micrographs were collected at various accelerating voltages (usually 5 – 20kV) and working distance values to optimize resolution, interaction volume, and X-ray signal intensities. The systems were calibrated and corrected for drifting conditions before starting every session to obtain reproducible results. By examining SEM-EDS images from both untreated and microwave-treated samples, the microstructural and elemental properties were assessed, such as texture at the micrometer or nanometer scale, thermally-induced cracking, and grain boundary separation due to differential microwave heating. Additionally, by observing how REEs are distributed among Fe-, Ti-, Si-, and Na-rich matrices, the qualitative information regarding improvements in the extraction of minerals from the RM samples by the application of microwave pre-treatment was obtained; this has implications for enhancing the efficiency of subsequent leach processes.

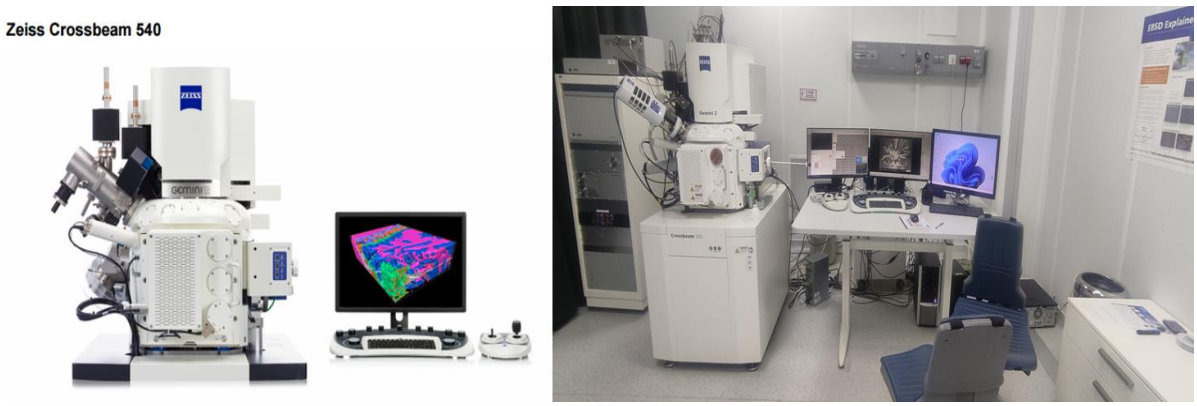

Figure 16. Zeiss Crossbeam 540 SEM–EDS (schematic (left) and laboratory setup (right)).

4.4.2 ATR-FTIR Spectrometer Analysis

FTIR analyses were performed on the Thermo Scientific Nicolet iS12 spectrometer that included an attenuated total reflectance (ATR) attachment consisting of a diamond crystal. ATR is useful as it provides constant physical interaction between the powdered red mud and the diamond crystal, allowing consistent and repeatable measurement of the red mud residues. The Nicolet IS line of instruments is capable of providing high S/N ratios, automatically corrects backgrounds, acquires spectra in real time, and maintains the interferometer in proper alignment; therefore, these instruments are well-suited for repetitive sampling. Each powdered KRM sample was simply pressed into the diamond crystal in such a way as to obtain good contact without applying excessive pressure. The OMNIC software provided the capability of viewing data in real time as each spectrum was acquired. The RM samples were analyzed over the mid-IR region from 4000 to 400 cm^{-1} with a resolution of 4 cm^{-1}. To increase the S/N ratio of the average spectrum, several scans were accumulated.

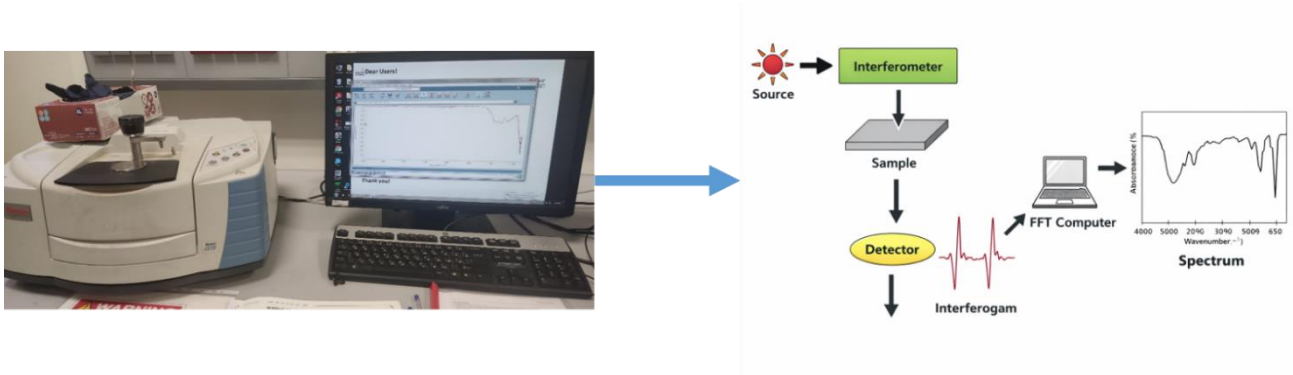

Figure 17. ATR-FTIR spectrometer (Thermo Scientific Nicolet iS12) and schematic of the FTIR measurement process.

4.4.3 Powder X-ray Diffraction (XRD) Analysis

Powder X-ray diffraction (XRD) analyses were performed on a Rigaku SmartLab multi-purpose diffractometer. The XRD measurements were made using the θ-θ arrangement as shown in Figure 18. This configuration provides the ability to measure phase composition and structural

characteristics from powder samples. It has two optical configurations: Bragg-Brentano and parallel beam; it also has automated sample alignment, as well as an extremely fast 2-D detector. Cu Kα X-rays (λ = 1.5406Å) were utilized as the X-ray source for this experiment. Each diffraction pattern was measured at a 2θ range of 10 – 80 degrees using a 5 degree per minute scan speed. In addition to the previously stated parameters, each set of experimental conditions was optimized based upon the specific needs of the analytical technique being employed. Interplanar spacing (d) of the material was determined by applying Bragg's law:

$$n\lambda=2d\sin\theta \qquad (3)$$

In Equation 2, 'n' represents the diffraction order, which was assumed to be equal to one for all measurements. 'λ' is the wavelength of the x-ray that was used in these experiments. 'θ' is the Bragg angle. Average particle diameters (D) of the synthesized TiO_2/Ti nanoparticles were estimated by utilizing the Debye-Scherrer equation**:**

$$D = \frac{K\alpha}{\beta cos\theta} \qquad (4)$$

Equation 3, 'K' represents the shape factor (typically taken to be approximately 0.9). 'β' represents the full-width at half-maximum (FWHM) of each peak. This value is represented in radians. 'θ' is the Bragg angle. The resulting diffraction patterns are compared to the reference files available in the Joint Committee on Powder Diffraction Standards (JCPDS) database in order to establish phase composition and evaluate crystalline structure.

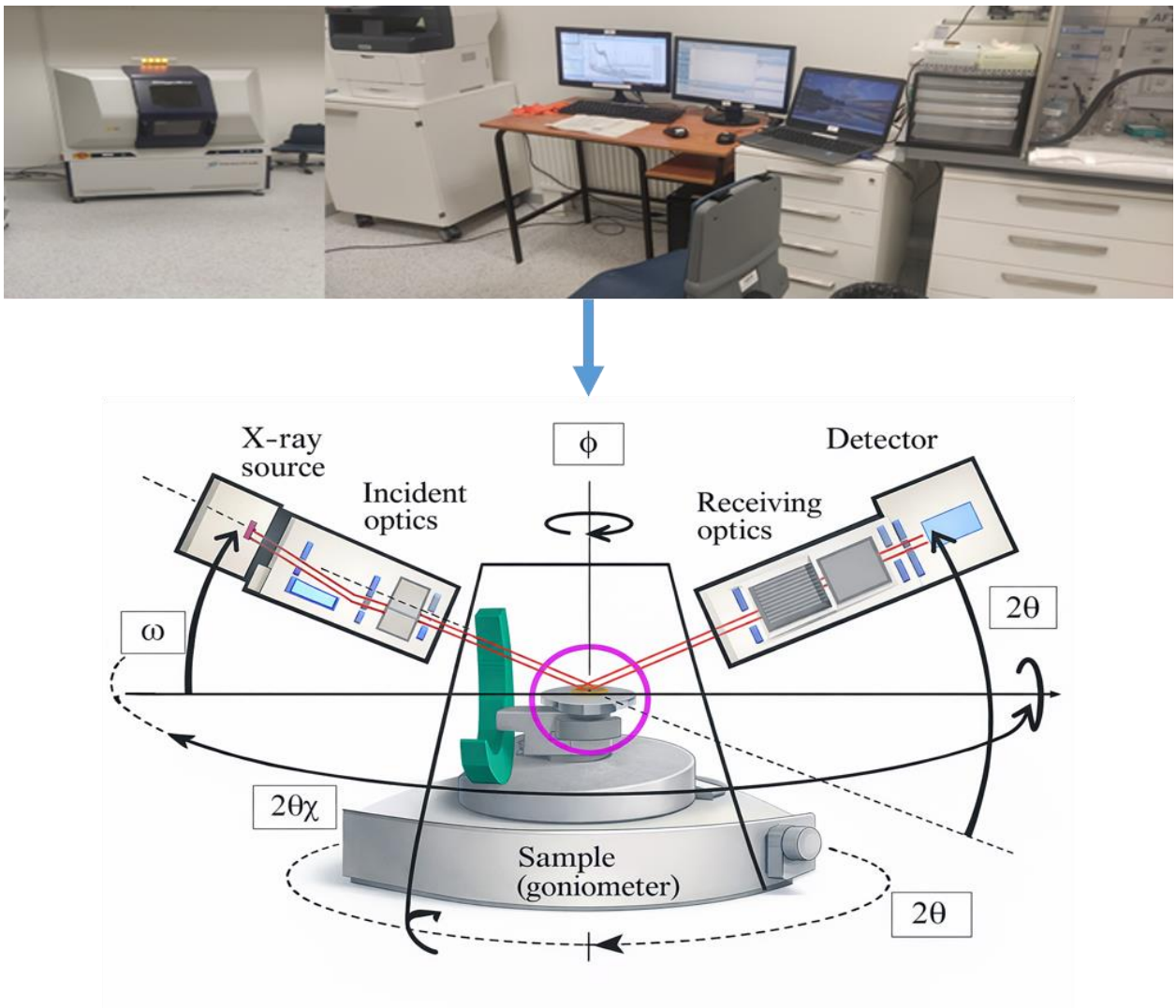

Figure 18. Rigaku SmartLab XRD setup used for phase identification and crystallographic analysis of red mud samples before and after microwave treatment.

4.4.4 ICP-OES Analysis

The Thermo Scientific iCap 6300 ICP-OES spectrometer (Figure 19) was used as the instrument to measure the elemental concentrations of both major and trace components of RM through the use of Inductively Coupled Plasma Optical Emission Spectroscopy (ICPOES) methods. All samples underwent digestion using appropriate amounts of an acid mixture so that all solids would be completely dissolved, followed by dilutions to obtain final solution concentrations for measurement. Standards consisting of Multi-Element Standard Solutions were used to calibrate the ICP-OES, and an internal standard solution was added to each sample to enhance both analytical accuracy and precision. The results from the ICP-OES analyses can provide quantitative elemental information to support evaluations of elemental concentrations and provide evidence of both leachability and recovery efficiencies.

Figure 19. Thermo Scientific iCAP 6300 ICP-OES.

4.4.5 XRF Analysis

In order to assess the total chemical composition of the KRM samples, X-ray fluorescence (XRF) spectroscopy was employed. A PANalytical Axios FAST wavelength dispersive type X-Ray Fluorescence (WDXRF) Spectrometer fitted with a Rh anode X-ray source was utilized for the analysis. Samples were initially dried in order to remove moisture; then they were finely powdered (<75μm); and finally each was compressed into a pellet as a means to achieve both the required homogeneity of the material and to produce results that could be reproduced. By determining the specific energy of the X-rays emitted by the elements contained in the sample, WDXRF spectroscopy can provide semi-quantitative or quantitative information concerning the relative amounts of major and minor oxides present in the sample. A calibration procedure was conducted using relevant standards, and the operating parameters of the instrument were optimized so that accurate analyses were achieved. The results of this analysis provided supporting evidence for further interpretations based on the mineralogy and geochemistry of the red mud samples.

4.5 Recovery Calculations

REE recovery (%) was calculated as:

$$Recovery = \frac{C_{Leachate} \times V}{m_{RM} \times C_{intial}} \times 100$$

Where:

- $C_{leachate}$= REE concentration in solution (ppm)
- V = volume of leachate (mL)
- m_{RM}= mass of red mud (g)
- $C_{initial}$ = initial REE concentration in RM (ppm)

Mass balance closure was verified within ±5%.

5 Results and Discussion

5.1 Main Characterization of Raw Red Mud

5.1.1 XRF analysis results

Chemical composition of the KRM sample was performed by X-ray Fluorescence (XRF), and the results are shown in Table 6. The sample consists mainly of Fe_2O_3(31.93 wt.%), Al_2O_3 (20.29 wt.%), and SiO_2 (17.17 wt.%), which corresponds to common RM containing iron oxides. Also, a relatively large amount of Na_2O (15.16 wt.%) was detected, which indicates residual alkalinity from the Bayer process. TiO_2 was found in minor concentrations (7.49 wt.%), which suggests the existence of titanium-bearing minerals like anatase or rutile. The presence of trace elements as well as potentially useful elements has been established. These include CaO (0.69 wt.%), V_2O_5 (0.052 wt.%), Ga_2O_3 (0.008 wt.%), and ZnO (0.023 wt.%). Total rare earth element content (ΣREE) of 0.371 wt.% (3,710 ppm) demonstrates significant potential for use of KRM as a secondary source for critical raw materials.

Table 6. Major oxide composition and elemental concentrations of red mud (KRM) determined by XRF analysis.

Compound / Formula	Conc. %	Oxide ppm	Element	Element in oxide %	Element ppm
Na_2O	15.158	151 580	Na	74.19	112 600
Al_2O_3	20.29	202 900	Al	52.93	107 400
SiO_2	17.17	171 700	Si	46.74	80 200
Fe_2O_3	31.93	319 300	Fe	69.94	223 400
TiO_2	7.49	74 900	Ti	59.93	44 900
CaO	0.69	6 900	Ca	71.47	4 940
V_2O_5	0.052	520	V	56.03	291
Ga_2O_3	0.008	80	Ga	74.40	60
ZnO	0.023	230	Zn	80.34	185
ΣREE	0.371	3 710	—	—	—

The presence of predominant Fe-, Al-, and Si-rich matrices suggests association of REEs with iron oxides and aluminosilicate matrices, which may hinder the leaching efficiency of these elements directly.

5.1.2 ICP-OES analysis for the presence of REEs in KRM sample

The REEs composition of the KRM sample was determined via ICP-OES, and the resulting values are listed in Table 7. Of all the evaluated elements, Neodymium (Nd) showed the largest quantity (1,420 ppm) as well as Cerium (Ce, 1,295 ppm). Erbium (Er), Samarium (Sm), and Praseodymium (Pr) were found to have moderate amounts of each respective element. Moreover, the presence of Scandium (Sc), which is a vital and very valuable mineral, was observed to be in large quantities (120 ppm). Dysprosium (Dy), Yttrium (Y), Gadolinium (Gd), and Lanthanum (La) were among other REEs observed to be in small amounts, and Lutetium (Lu) and Terbium (Tb) had concentrations below LOQ. This shows that the rare earth minerals contained high amounts of Light Rare Earth Elements (LREEs) and relatively low amounts of Heavy Rare Earth Elements (HREEs). The Full REE Distribution can be seen in Table 7. However, because of the significance of the four studied REEs and their large enough quantities to be relevant to the leach experiments, Ce, Nd, Sm, and Eu will be used for additional study. This data confirms that KRM has both measurable and economically viable concentrations of REEs, specifically Nd and Ce. The presence of LREEs in larger numbers than HREEs, along with the fact that these LREEs associate with most of the major mineral phases, indicates that the effectiveness of microwave-assisted treatment in extracting them from the RM would depend on the mineralogy of the RM matrix.

Table 7. Rare earth element (REE) concentrations in KRM, determined by ICP-OES analysis.

Element	Conc. %	ppm
Ce	0.1295	1 295
Dy	0.0096	96
Er	0.0202	202
Eu	0.0015	15
Gd	0.0073	73
Ho	0.0016	16
La	0.0046	46
Lu	h/o	< LOQ
Nd	0.1420	1 420
Pr	0.0140	140
Sc	0.0120	120
Sm	0.0185	185
Tb	h/o	< LOQ
Tm	0.0035	35
Y	0.0064	64

5.2 SEM–EDS Analysis of KRM sample

As shown in Figure 20, the SEM images of KRM show an aggregate structure with dense aggregation of small, fine, angular fragments. A characteristic feature of this type of RM is the high density of surface irregularities and roughness. These morphological characteristics result from the presence of various iron oxide, titanium, and aluminosilicate minerals in the structure. Surface fragmentation and surface irregularity can lead to an increase in the reactive properties of the surface. In accordance with the SEM images, the EDS spectrum shows significant peaks for the primary components, i.e., Fe, Al, Ti, and O. These correspond to data obtained using X-ray fluorescence (XRF) and X-ray diffraction (XRD).

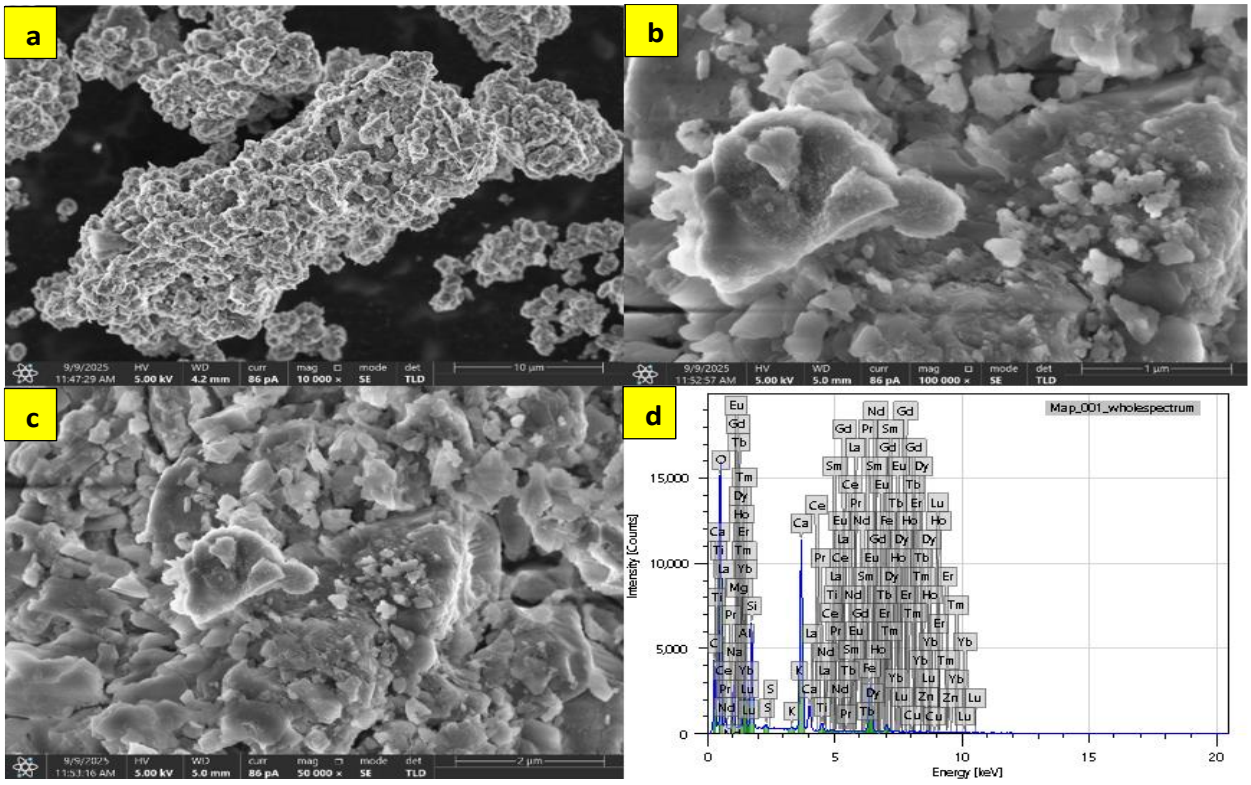

Figure 2. SEM micrographs (a-c) with varying magnifications and (d) corresponding EDS spectrum of the KRM sample.

The elemental map of the KRM sample (SEM-EDS) from Figure 21 showed that all the main components (Fe, Al, Si, Ti, Na, and Ca) are relatively uniformly distributed over the area examined. However, both the intensity of iron and titanium were significantly higher than those of other components. This confirms that the Fe-Ti bearing minerals dominate the composition of the sample as indicated by XRF and XRD analyses. Aluminium and Silicon are equally distributed throughout the matrix. Thus, it can be assumed that there is an equal proportion of aluminium silicate phases present in the matrix.

The mapping of the traces for the Rare Earth Elements (Nd, Ce, Dy, Sm, and Y) has shown that these trace elements have very weak and homogenously distributed signals. No areas of high concentrations could be identified. Therefore, it can be concluded that these rare earth elements are finely dispersed throughout the matrix and are probably bound to either iron oxide and/or titanate phases, as well as being incorporated into amorphous aluminosilicate phases. It does not appear to occur as discrete grains.

Thus, it appears that the recovery of the rare earth elements is primarily dependent upon processes occurring within the matrix and thus will depend upon the liberation of the relevant phase and its diffusional characteristics rather than purely physical separation.

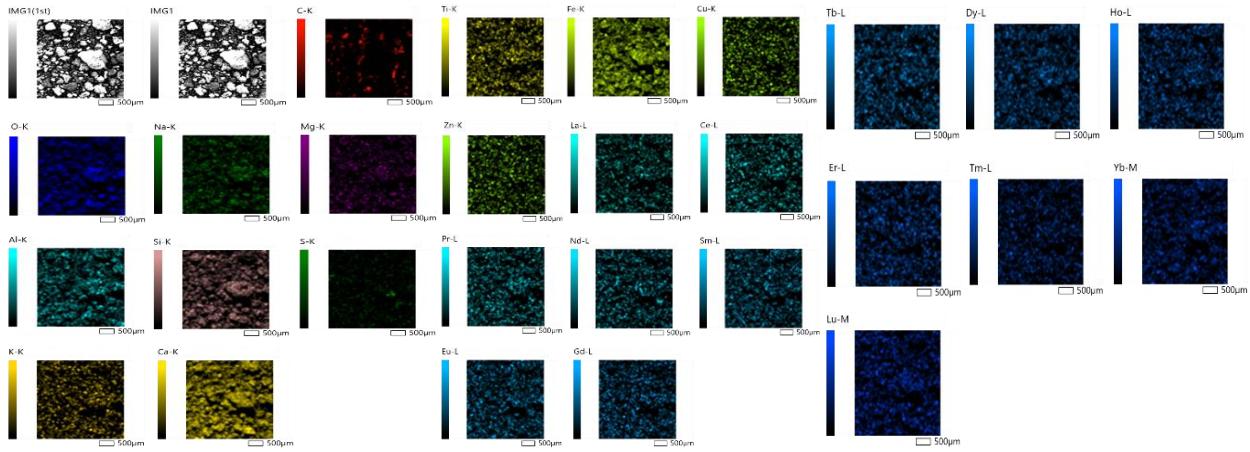

Figure 21. SEM–EDS elemental mapping of the KRM sample illustrating the spatial distribution of major elements and trace REEs.

The SEM images of KRM appear to contain an uneven but somewhat dense structure that consists of several sharp-edged particles. These have many large peaks and valleys on their surfaces. In comparison to TRM, KRM seems to be denser and has sharper boundaries between each particle; this would also explain why there is less accumulation of small particles due to heat treating. It can also account for some degree of sintering as well as the possibility of phase changes which could be related to the increase in crystalline order as indicated by the XRD data. The elemental distribution and concentration (in weight percent) from the EDS analysis (Table 8) shows a relatively even distribution among all of the major elements such as Fe, Al, Si, Ca, Na and Ti. The primary element present is iron, which supports that most of the phases are primarily iron oxides. Aluminum and silicon are found with aluminosilicate and remaining alumina phases. Although calcium levels seem higher than expected, it may suggest that Ca-containing phases were formed or redistributed during processing. Moderate amounts of titanium were identified, however it was

spread out relatively evenly throughout the sample, which suggests that the TiO_2-containing phases are randomly dispersed throughout the sample.

Table 8. SEM–EDS elemental mapping of the KRM sample illustrating the spatial distribution of major elements and trace REEs.

Element	Line	Mass %	Atom %
C	K	17.48 ± 0.06	27.76 ± 0.09
O	K	43.68 ± 0.14	52.08 ± 0.16
Na	K	4.40 ± 0.05	3.65 ± 0.04
Mg	K	0.27 ± 0.02	0.21 ± 0.02
Al	K	3.20 ± 0.03	2.27 ± 0.02
Si	K	4.90 ± 0.03	3.33 ± 0.02
S	K	0.18 ± 0.01	0.11 ± 0.00
K	K	0.09 ± 0.01	0.04 ± 0.00
Ca	K	14.34 ± 0.05	6.83 ± 0.03
Ti	K	0.81 ± 0.02	0.32 ± 0.01
Fe	K	9.33 ± 0.06	3.19 ± 0.02
Cu	K	0.20 ± 0.02	0.06 ± 0.01
Zn	K	0.16 ± 0.02	0.05 ± 0.01
La	L	0.00 ± 0.02	0.00 ± 0.00
Nd	L	0.03 ± 0.02	0.00 ± 0.00
Sm	L	0.05 ± 0.02	0.01 ± 0.00
Eu	L	0.09 ± 0.02	0.01 ± 0.00
Tb	L	0.36 ± 0.04	0.04 ± 0.01
Dy	L	0.30 ± 0.04	0.04 ± 0.01
Ho	L	0.12 ± 0.03	0.01 ± 0.00
Total		**100.00**	**100.00**

The SEM-EDS analysis data indicate that the RM sample has high amounts of oxygen (43.68 wt%) and carbon (17.48 wt%). High levels of oxygen and carbon in the sample indicate that oxides and carbonates exist within the sample. There are also high levels of additional minerals in the sample, particularly an abundance of calcium (14.34 wt%), indicative of large quantities of the mineral calcite. Moderate to low levels of aluminum have been found in the red mud samples (3.2 wt%), and may be related to either the silica-bearing minerals or the aluminosilicate matrix. Besides these materials, the RM samples contained trace amounts of sodium (4.4 wt%) that could come from

remaining alkaline solutions utilized throughout the Bayer process. Additionally, minor elements were identified in the red mud samples, including titanium (0.81 wt%), magnesium (0.27 wt%), sulfur (0.18 wt%), copper (0.20 wt%), and zinc (0.16 wt%). REEs, such as neodymium (0.03 wt%), samarium (0.05 wt%), europium (0.09 wt%), terbium (0.36 wt%), dysprosium (0.30 wt%), and holmium (0.12 wt%), were detected at very low concentrations (≤0.4 wt%), which is consistent with the known enrichment of REEs in bauxite residues and suggests potential for their recovery. However, several REEs, including Ce, Gd, Er, Tm, Yb, and Lu, were below the detection limit.

5.3 FTIR Analysis of KRM sample

The FT-IR spectrum of KRM sample is presented in Figure 22. Many peaks represent all the major constituents present in a typical RM. The peak at 980–1000 cm^{-1} can be assigned to the Si-O stretching vibration, indicating the presence of both silicate and aluminosilicate phases. The peak between 1400–1500 cm^{-1} is a CO_3^{2-} group peak; it appears that these have developed after storage/processing of the samples as a result of carbonation. The peak between ~1630 cm^{-1} was very weak and can be assigned to H-O-H bending. Also, the broad peak between 3400–3600 cm^{-1} is associated with O-H stretching, showing the presence of adsorbed water on the surface of the minerals and hydroxyl-bearing minerals.

Therefore, the overall data indicate that the RM sample is an amorphous mixture of a number of different minerals. These include silicate, carbonate, and hydroxyl phases. The carbonate component will consume acid when exposed to an acidic environment, therefore reducing the leachability of other components; however, the hydroxyl-bearing phases may increase their reactivity with acid. Conversely, the silicate phases are capable of encapsulating rare earth elements (REEs) into their structures, thus limiting their availability for direct extraction. This is consistent with the XRF and SEM-EDS data, where REEs were shown to be entrapped in a complex matrix. Due to the above reasons, pre-treatment techniques, e.g., microwave activation, are necessary to break down the matrices so that leaching can occur effectively.

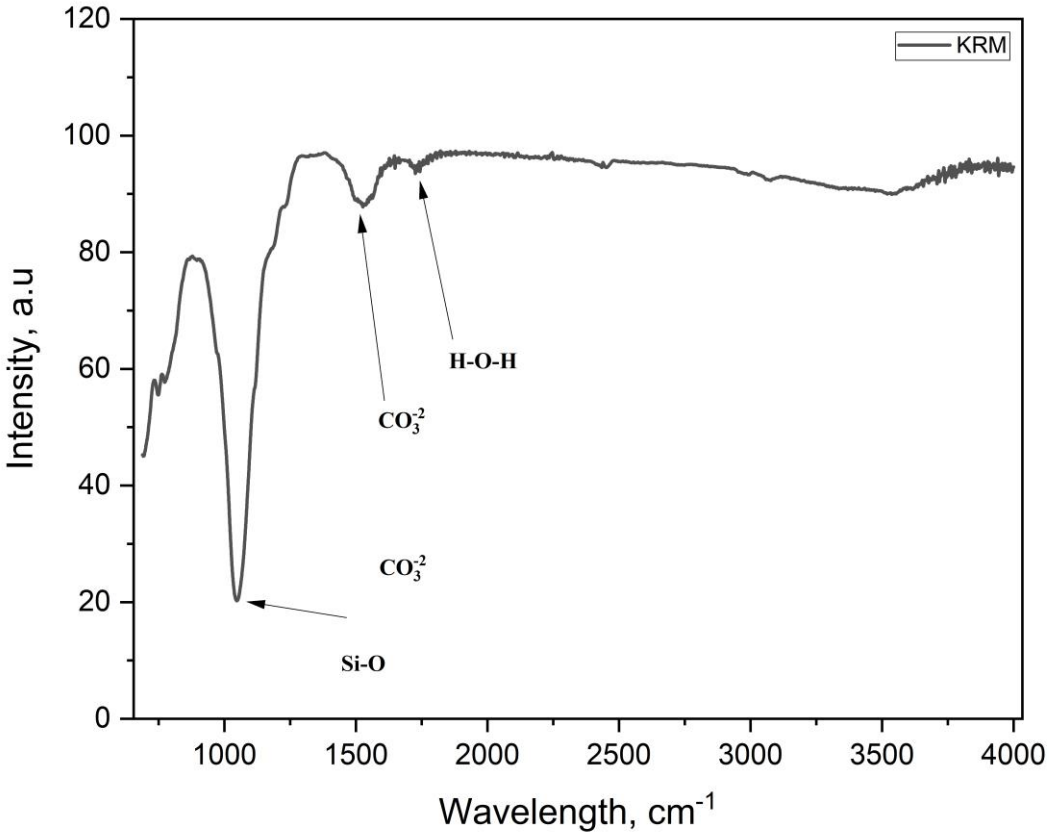

Figure 22. FTIR spectrum of the KRM sample.

5.4 XRD Analysis of KRM sample

The XRD spectrum of the KRM is presented in Figure 23, which shows multiple crystalline phases in addition to a complex mineral matrix. The identified peaks correspond to gibbsite/boehmite (G), hematite (H), anatase (A), quartz (Q), and rutile (R), indicating that the sample consists of Fe-, Al-, Si-, and Ti-bearing phases. The large peak at about 25° (2θ) indicates the presence of anatase (TiO_2); thus, titanium-bearing phases are confirmed from the XRF data. Large peaks in the ranges of 33–36° and 49–55° show the presence of hematite (Fe_2O_3), indicating iron oxides dominate this sample. Other peaks for quartz (~26.6°) further indicate silicate phase presence, while additional peaks from rutile confirm titanium mineral presence. The low-angle features for gibbsite/boehmite indicate aluminum hydroxide phases typical of bauxite residue. Sharp diffraction peaks and high background indicate both crystalline and amorphous components in this sample; the amorphous portion can be assumed to be related to the aluminosilicate phases. Therefore, the prevalence of Fe–Ti bearing phases combined with the presence of silicates and minor quartz verifies that KRM is heterogeneous/multiphase. In fact, the mineralogical structure is consistent with SEM–EDS data showing REEs are embedded in the matrix rather than present as discrete phases. Hence, the extraction of these REEs is likely controlled by structural encapsulation & diffusion limitations,

highlighting the importance of pretreatment methods such as microwave activation to increase accessibility between phases and improve leachability.

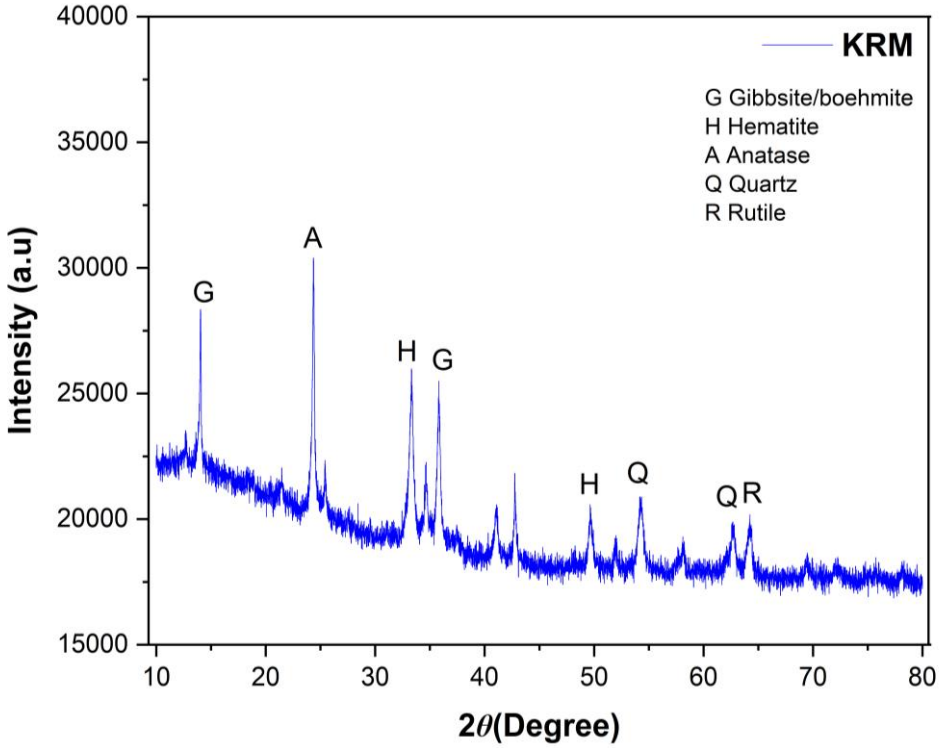

Figure 23. X-ray diffraction (XRD) pattern of the KRM sample (Cu Kα radiation, 2θ = 10–80°), showing the presence of gibbsite/boehmite (G), hematite (H), anatase (A), quartz (Q), and rutile (R) phases.

5.5 Leaching System and Sample Preparation

Leaching experiments were conducted in an orbital laboratory scale shaker, which provides well-defined agitation and constant temperature at 90°C. This orbital shaker maintains a continuously mixed solid–liquid slurry, so that the interaction between the RM particles and the leaching solution can be maintained throughout the experiment. This method allows uniform reaction conditions to be maintained and minimizes any mass transfer limitation during the leaching process.

Figure 24. Laboratory orbital shaking incubator used for controlled chemical leaching experiments at 90 °C with regulated agitation speed.

The following six experiments were run in the course of this investigation. These included three Microwave-Assisted Leaching (MT+L) experiments and three Direct Leaching (DL) experiments. The experiments that were run in this research utilized the same three types of acids, which are H_2SO_4 (Sulfuric Acid), HNO_3 (Nitric Acid), and HCl (Hydrochloric Acid), in an attempt to determine the effect of acid type as well as microwave pretreatment on the extraction of Rare Earth Elements (REEs).

Three DL experiments were performed utilizing the three acid systems (same as MT+L experiments); however, no pre-treatment was applied prior to the leaching process. In contrast, the RM samples in the MT+L experiments were first treated using microwaves (1500W for 60 min.), then the sample was subjected to leaching under the same chemical and thermal conditions as the DL experiments. This provided a method for determining whether or not microwave treatment had an impact on the ability to extract REEs.

After each experiment, the leachate solution suspensions were separated from the solid phase by centrifugation. Once separated, they were further processed by filtering to produce clear leachate solutions (Figure 25).

Figure 25. Centrifugation step used for solid–liquid separation of leachate samples prior to ICP-OES analysis.

As indicated in Figure 26, representative liquid fractions produced from the different acid systems can be visually distinguished based on their color intensity and turbidity. The two acid systems that produced the darkest reddish brown colors were the sulfuric acid (SA) and nitric acid (NA) systems. The hydrochloric acid (HA) system produced significantly lighter colored leachate solutions than did the other two systems.

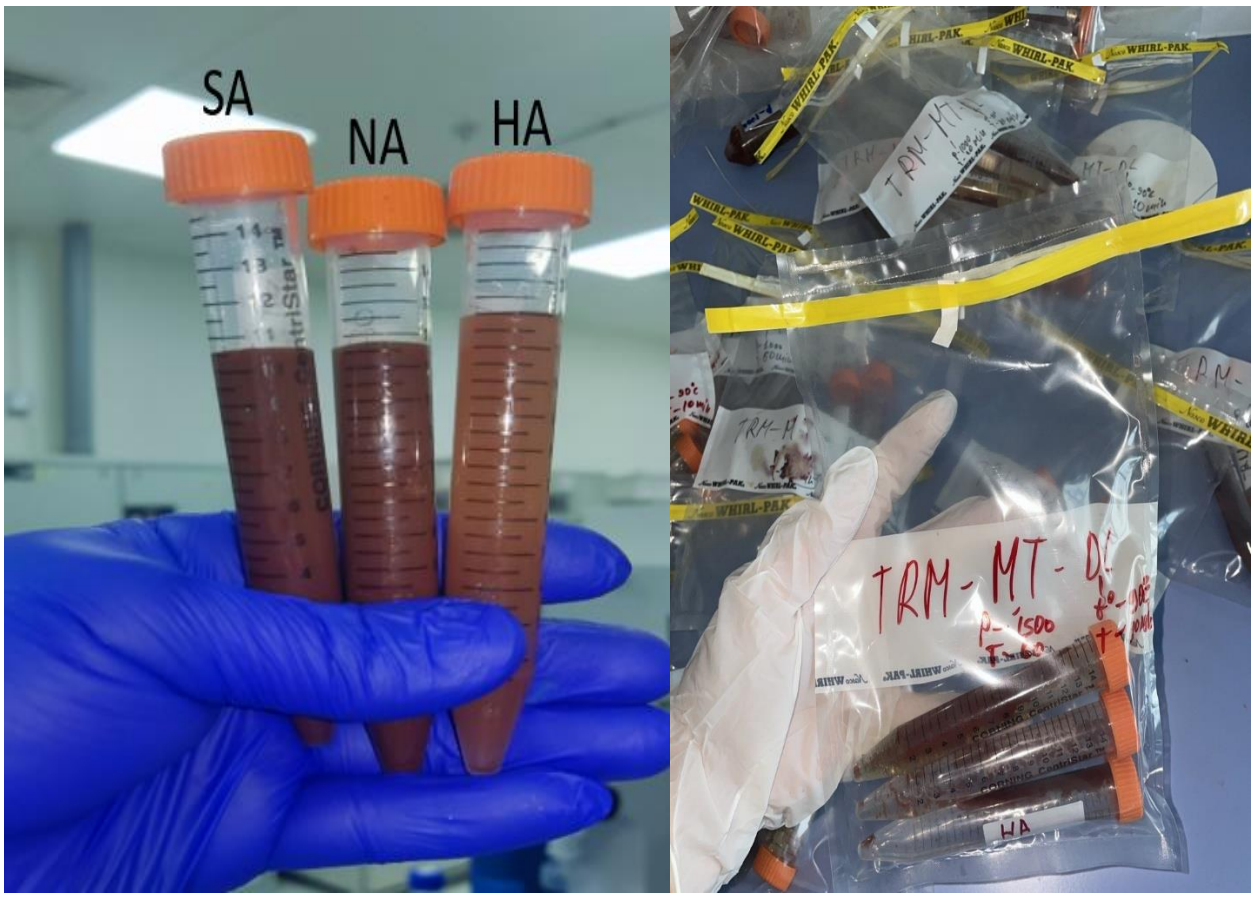

Figure 26. Representative leachate solutions obtained after microwave-assisted chemical leaching of KRM using sulfuric (SA), nitric (NA), and hydrochloric (HA) acid.

Visual observations suggest that a darkening coloration exists in the SA and NA systems compared to the HA system. This observation is generally attributed to an increase in the amount of iron-bearing phases such as hematite that are being dissolved, with the Fe^{3+} ions from these phases increasing the solution color due to their ability to form soluble complexes. Therefore, it can be concluded that there are likely to be significant differences in the way metals dissolve and possibly in the solution chemistry or in the mechanism of complexation among the three systems studied. It also appears that both sulfate and nitrate systems may favor the dissolution of primary components of the matrix of the feed material examined, whereas the chloride system does not appear to have the same preference for dissolution. Although qualitative data cannot be obtained by comparing colors of solutions, the qualitative evidence that was determined will serve as a basis for determining whether the REEs could be recovered based on chemical analysis performed on the leachate. All three separate solutions were further filtered to remove any additional particulate matter that could interfere with the clarity and accuracy of results obtained during ICP-OES analysis. Additionally, all three solutions were diluted (25 times) with deionized water so that the concentration of each element analyzed would fall within the calibration limits of the ICP-OES instrument used for this study. Diluting samples to achieve desired concentrations provides

protection against potential matrix effects.

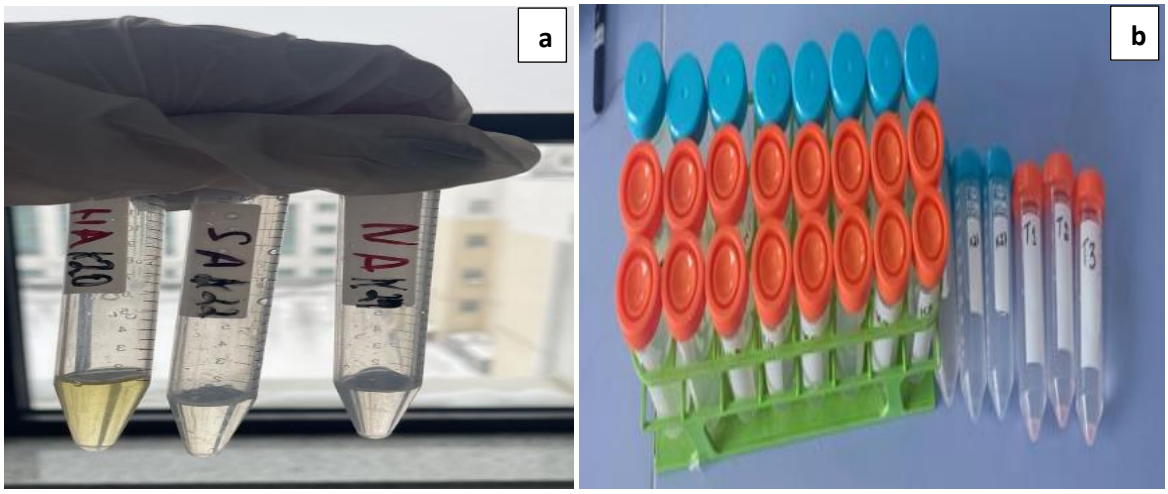

Figure 27. Leachate samples after solid–liquid separation and dilution for ICP-OES analysis: (a) filtered solutions, and (b) diluted samples (25×).

5.6 KRM sample Leaching (DL vs MT+L)

The results of direct leaching (DL) and microwave-assisted leaching (MT+L) for selected REEs (Ce, Nd, Sm, and Eu) are presented in Tables 9–12.

Table 9. Comparison of cerium (Ce) concentration and extraction efficiency obtained from direct leaching (DL) and microwave-assisted leaching (MT+L) using different acid systems.

Sample	Acid	Type	Ce (ppm)	Ce extraction (%)
S1	Sulfuric	DL	0.01062	0.34
S2	Sulfuric	MT+L	0.02934	0.94
H1	Hydrochloric	DL	0.00894	0.29
H2	Hydrochloric	MT+L	0.13551	4.36
K1	Nitric	DL	0.01178	0.38
K2	Nitric	MT+L	0.02573	0.83

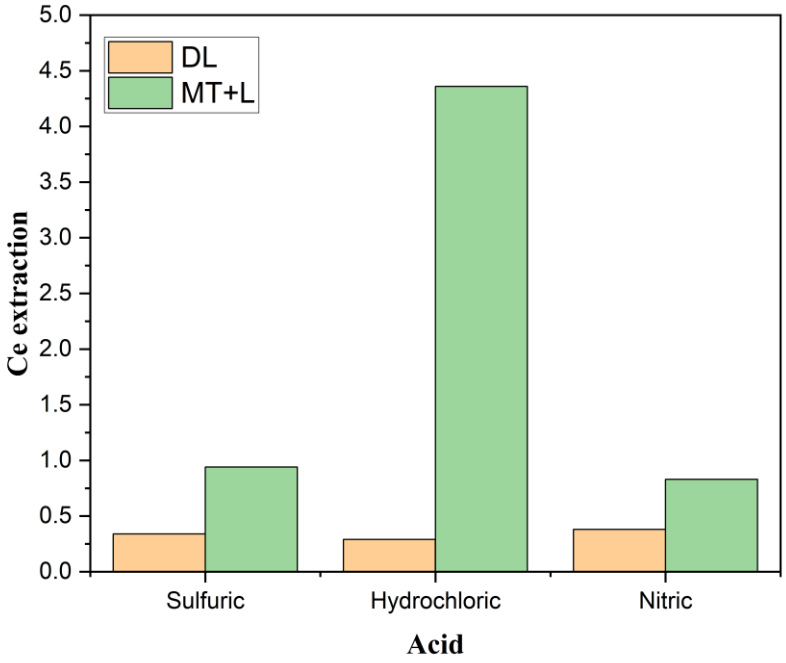

Figure 28. Ce recovery under different leaching conditions.

Table 10. Comparison of neodymium (Nd) concentration and extraction efficiency for DL and MT+L experiments under sulfuric, hydrochloric, and nitric acid systems.

Sample	Acid	Type	Nd (ppm)	Nd extraction (%)
S1	Sulfuric	DL	0.00465	0.14
S2	Sulfuric	MT+L	0.01208	0.35
H1	Hydrochloric	DL	0.00395	0.12
H2	Hydrochloric	MT+L	0.11921	3.50
K1	Nitric	DL	0.00549	0.16
K2	Nitric	MT+L	0.01083	0.32

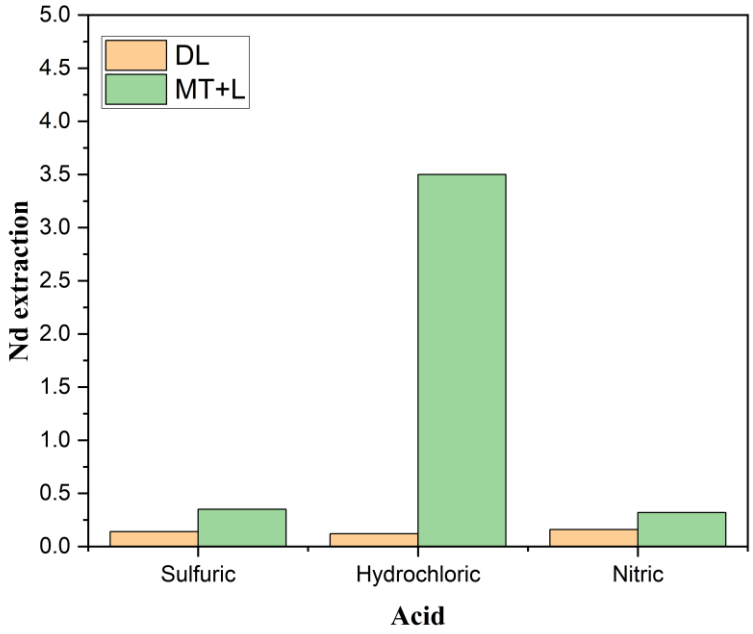

Figure 29. Nd recovery under different leaching conditions.

Table 11. Comparison of samarium (Sm) concentration and extraction efficiency obtained from DL and MT+L processes for different acid systems.

Sample	Acid	Type	Sm (ppm)	Sm extraction (%)
S1	Sulfuric	DL	0.00104	0.23
S2	Sulfuric	MT+L	0.00254	0.57
H1	Hydrochloric	DL	0.00083	0.19
H2	Hydrochloric	MT+L	0.02229	5.02
K1	Nitric	DL	0.00123	0.28
K2	Nitric	MT+L	0.00227	0.51

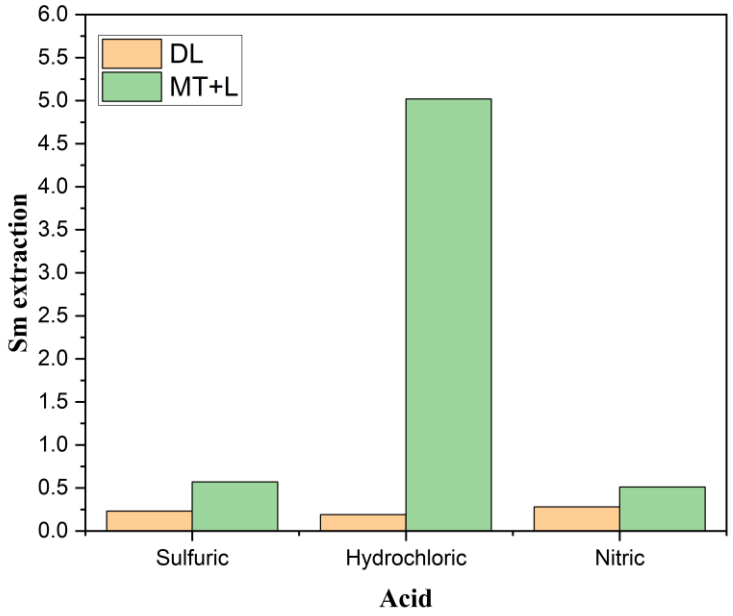

Figure 30. Sm recovery under different leaching conditions.

Table 12. Comparison of europium (Eu) concentration and extraction efficiency for direct (DL) and microwave-assisted leaching (MT+L) under different acid conditions.

Sample	Acid	Type	Eu (ppm)	Eu extraction (%)
S1	Sulfuric	DL	0.00029	0.79
S2	Sulfuric	MT+L	0.00069	1.92
H1	Hydrochloric	DL	0.00024	0.67
H2	Hydrochloric	MT+L	0.00494	13.71
K1	Nitric	DL	0.00036	1.00
K2	Nitric	MT+L	0.00060	1.67

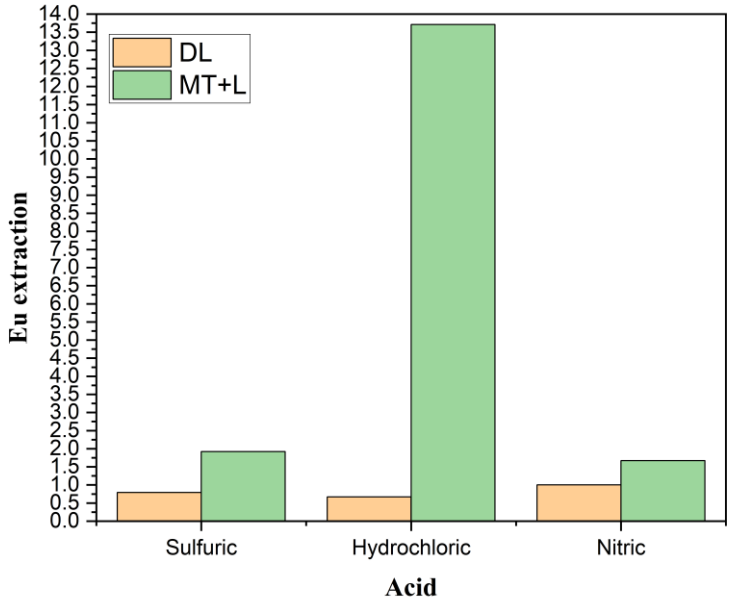

Figure 31. Eu recovery under different leaching conditions.

A comparison of direct leaching (DL) and microwave-assisted leaching (MT + L) indicates a positive influence of microwave pre-treatment on the recovery of Rare Earth Elements (REEs). All four studied REE (Ce, Nd, Sm, and Eu) were extracted at greater efficiencies using MT + L than by using DL under identical chemical conditions. The greatest increase in extraction rates was realized with HCl; extraction values for both Ce and Nd, in particular, were greatly enhanced. Extraction increases were also seen with both H_2SO_4 and HNO_3, but they were much less pronounced than those obtained with HCl. Although the general trend indicated an improvement in the extraction rate for all the studied REE, Sm and Eu generally had lower extraction rates than Ce and Nd, suggesting a greater association of Sm and Eu with the less reactive mineral phases present in the RM. It is likely, therefore, that the increased efficiency of MT + L over DL arises from microwave-induced physical changes to the RM, i.e., micro-cracking and increased accessibility to phases containing the REEs, facilitating their dissolution into solution.

5.7 SEM analysis of the leached KRM sample

The microstructure of KRM samples before and after microwave-assisted leaching was analyzed using SEM analysis, as depicted in Figure 32. Prior to treatment, the heterogeneous aggregated structure of the sample was composed of fine irregular particles; following treatment, structural changes were observed within the particle fragments as well as surface cracking and partial re-organization. The formation of micro-cracks due to thermal stress induced by the microwave pretreatment contributed to the weakening of the particulate structure. Lamellar plate-like morphologies were also observed in some regions, suggesting possible recrystallization or phase transformation. The improved accessibility of internal surfaces and enhanced diffusion into the particle matrix resulted from these structural modifications. However, dense fine particles remain present, suggesting that certain phases are resistant to dissolution. Overall, the results from the SEM analysis demonstrate a significant increase in reactivity of red mud and enhance its ability for leaching.

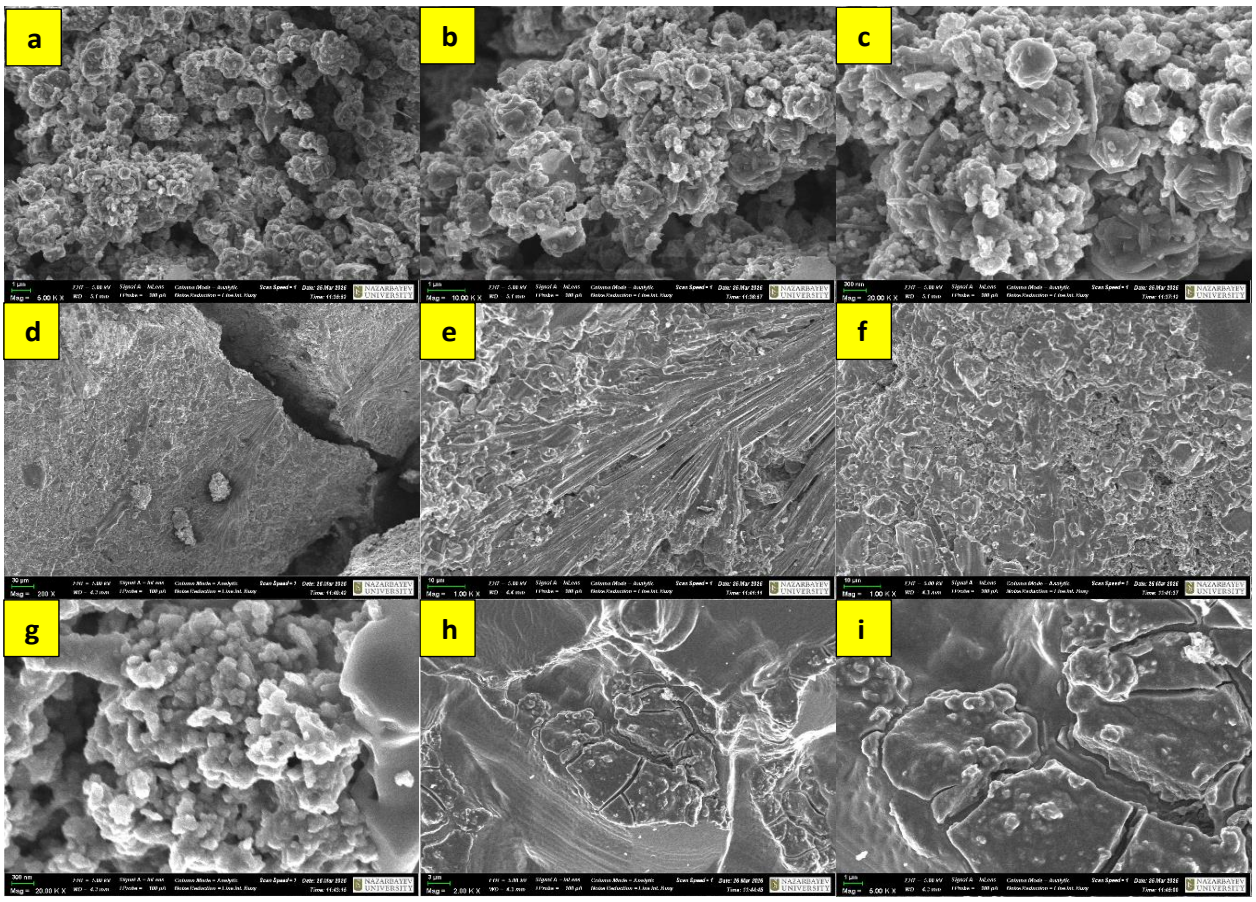

Figure 32. SEM micrographs of KRM samples before (a–c) and after (d–i) microwave-assisted leaching, showing morphological changes including particle fragmentation, surface cracking, and structural reorganization.

5.8 XRD Analysis of Red Mud after Leaching

RM samples that were subjected to microwave-assisted leaching (MT+L) versus those subjected to direct leaching (DL) have been evaluated with respect to their XRD pattern, as shown in Figure 33. The data provided confirm the presence of Quartz (Q), Hematite (H), Gibbsite/Boehmite (G), Anatase (A), and Rutile (R). As indicated previously, this data clearly illustrates that the KRM is a multi-phase material. A comparison of the DL and MT+L XRD patterns indicates that the Quartz peak in the DL sample was strong at approximately $2\theta \approx 26°$. The silica-rich phases appear to be relatively unaltered by leaching and therefore do not contribute significantly to the amount of extractable metals. Weak Hematite and Anatase peaks indicate only minor amounts of structural modification or release of the Fe- and Ti-containing minerals present. Similarly, the Gibbsite/Boehmite peaks indicate little alteration to the existing mineral structure when using DL. However, as can be seen from the MT+L XRD patterns, there appears to be a significant enhancement of the structural organization and degree of structural modification resulting from the application of microwave energy prior to DL. The improved definition and increased intensities of these peaks for Hematite and Gibbsite/Boehmite reflect improved crystallinity and possibly the

redeployment of minerals phases as a result of the thermal stresses created within the red mud matrix by microwave heating. The results obtained herein also illustrate how the improved metal recovery efficiencies observed in the MT+DL experiments can be attributed to microwave-assisted degradation of the red mud matrix, leading to greater accessibility of REE-containing phases. Thus, it is concluded that improved metal recoveries observed in MT+L experiments are a direct result of structural modifications occurring in the RM matrix as a consequence of microwave heating.

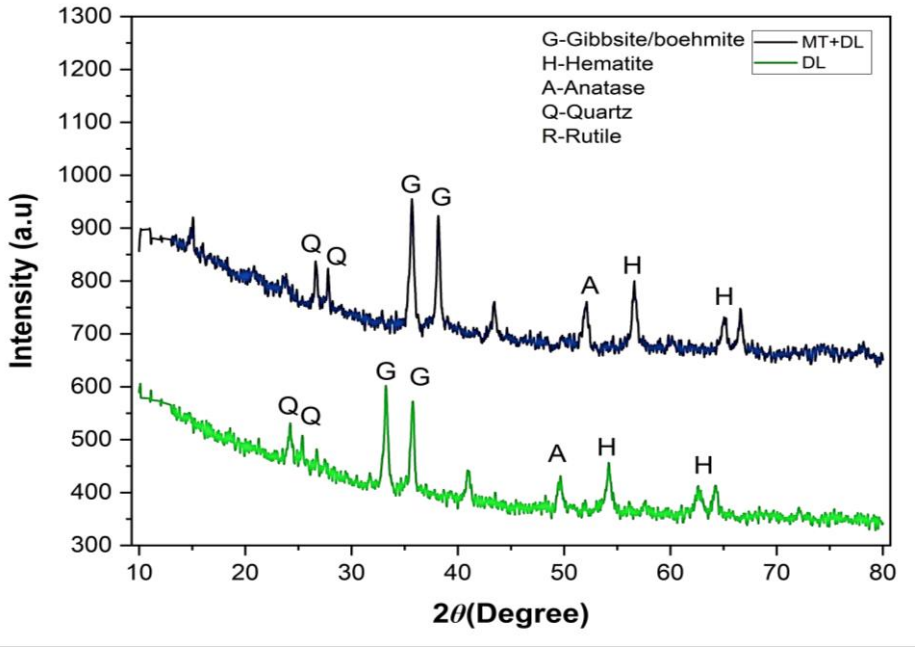

Figure 33. Comparative XRD patterns of red mud samples after direct leaching (DL) and microwave-assisted leaching (MT+DL), showing the presence of quartz (Q), hematite (H), gibbsite/boehmite (G), anatase (A), and rutile (R) with improved crystallinity.

The use of microwave-assisted pretreatment in the extraction of rare earth elements has shown that red mud valorization can be used to reduce the need to store large volumes of industrial waste through the recovery of valuable elements. This process also supports circular economy principles by utilizing red mud as a secondary resource instead of depending on primary raw materials. Although this study was limited to laboratory-scale experiments, it shows that there are opportunities for microwave-assisted processing to be used as a step towards more environmentally efficient and resource-oriented treatment of bauxite residue.

6 Conclusions and Recommendations

The effects of microwave-assisted pre-treatment on the extraction of rare-earth elements (REEs) from Kazakh Red Mud (KRM) have been studied in detail, along with the advantages of the microwave-assisted pretreatment over direct leaching. Microwave pre-treatment improved the leaching performance significantly due to the physical and chemical changes that occurred in the

material during microwave treatment. These changes include micro-crack formation and redistribution of mineral phases, along with the destruction of particles that facilitate the access of REEs originally enclosed in the iron oxides, aluminosilicate, and titanium-bearing phase. Experiments were conducted at 90°C utilizing sulfuric acid, nitric acid, and hydrochloric acid. Directly leached KRM exhibited lower extraction percentages than those obtained when microwave-assisted leaching was employed, particularly for Ce and Nd. However, Sm and Eu were extracted in low amounts in both cases because they are associated with highly resistant mineral phases. Additionally, the dependence of system behavior on mineralogical composition confirms that structure is a key factor influencing extraction efficiency. In summary, microwave pre-treatment enhances the REEs recovery through modification of the internal structure of RM and enhancement of diffusional processes during leaching, thus providing a valuable alternative for the valorisation of RM as a secondary source of critical materials. Nevertheless, some improvements are necessary, and therefore future works should aim to optimize the operating parameters of the process, such as microwave power, treatment time, and leaching conditions, as well as investigate in greater detail the interaction between microwave and material to gain deeper insight into structural changes and their consequences on leaching behavior.

7 References

[1] K. Evans, “The history, challenges, and new developments in the management and use of bauxite residue,” *J. Sustain. Metall.*, vol. 2, no. 4, pp. 316–331, 2016.

[2] L. Wang, N. Sun, H. Tang, and W. Sun, “A review on comprehensive utilization of red mud and prospect analysis,” *Minerals*, vol. 9, no. 6, p. 362, 2019.

[3] A. Akcil, K. R. Swami, R. L. Gardas, E. Hazrati, and S. Dembele, “Overview on hydrometallurgical recovery of rare-earth metals from red mud,” *Minerals*, vol. 14, no. 6, p. 587, 2024.

[4] E. E. Çelebi, “Determination of metal fractions and rare earth anomalies in red mud: the case of bauxite mining district of Seydişehir (Turkey),” *Environ. Earth Sci.*, vol. 83, no. 3, p. 93, 2024.

[5] B. Swain, A. Akcil, and J. C. Lee, “Red mud valorization an industrial waste circular economy challenge; review over processes and their chemistry,” *Crit. Rev. Environ. Sci. Technol.*, vol. 52, no. 4, pp. 520–570, 2022, doi: 10.1080/10643389.2020.1844563.

[6] M. Al-Harahsheh and S. Kingman, “Microwave-assisted leaching—A review,” *Hydrometallurgy*, vol. 73, pp. 189–203, 2004.

[7] R. K. Amankwah, C. A. Pickles, and W. T. Yen, “Improved grindability of minerals by microwave heating,” *Miner. Eng.*, vol. 18, pp. 1–5, 2005.

[8] X. Liu et al., “Microwave-assisted carbothermal reduction of red mud for enhanced Fe/Ti recovery,” *J. Clean. Prod.*, 2020.

[9] R. Singh et al., “Microwave processing of red mud for metal recovery,” *Miner. Eng.*, 2019.

[10] Y. Ma, C. Hu, Y. Jin, H. Zhen, J. Wu, and L. Yang, “Recovery of ruthenium resources from red mud via phosphoric acid leaching: A comprehensive investigation of leaching effects and kinetics,” *J. Clean. Prod.*, vol. 486, p. 144423, 2025, doi: 10.1016/j.jclepro.2024.144423.

[11] M. Widyaningsih, A. Mudzakir, F. Khoerunnisa, and B. S. Ooi, “Betaine-cis-oleic acid based eutectic ionic liquids as green solvent for recovery of rare earth elements from red mud,” *Total Environ. Eng.*, vol. 2, p. 100003, 2025, doi: 10.1016/j.teengi.2024.100003.

[12] E. Schingaro *et al.*, “Exploring the potential of red muds from Portovesme (SW Sardinia, Italy): Multiscale analysis of REEs content and mineralogy,” *Heliyon*, vol. 11, no. 9, 2025.

[13] Z. Ilkhani, F. Vakilchap, N. Sadeghi, and S. M. Mousavi, “Base metals (Fe, Al, Ti) and rare earth elements (Ce, La, Pr) leaching from red mud through an efficient chemical-biological hybrid approach,” *Miner. Eng.*, vol. 208, p. 108603, 2024, doi: 10.1016/j.mineng.2023.108603.

[14] P. Du, P. Wang, X. Zhang, G. Wen, and Y. Wang, “Properties, hazards and valuable metal recovery technologies of red mud: A review,” *Particuology*, vol. 93, pp. 328–348, 2024.

[15] S. Li, Z. Guo, J. Pan, D. Zhu, T. Dong, and S. Lu, “Extracting Al$_{2}$O$_{3}$ and TiO$_{2}$ from Red Mud Smelting Separation Slag by Alkali and Acid Leaching Methods,” *Metals (Basel).*, vol. 13, no. 3, p. 552, 2023.

[16] A. Cozzolino, “Extraction and recovery of valuable elements from red mud through biohydrometallurgy,” Ph.D. dissertation, University of Cagliari, Italy, 2023.

[17] I. V Loginova and A. V Kyrchikov, “The study of the magnetic properties of red mud from

alumina production after alkaline treatment," *Solid State Phenom.*, vol. 316, pp. 673–677, 2021, doi: 10.4028/www.scientific.net/SSP.316.673.

[18] J. S. Kim, N. C. Choi, and H. Y. Jo, "Selective Leaching Trace Elements from Bauxite Residue (Red Mud) without and with Adding Solid NH$_{4}$Cl Using Microwave Heating," *Metals (Basel).*, vol. 11, no. 8, p. 1281, 2021.

[19] D. Zinoveev *et al.*, "Research on high-pressure hydrochloric acid leaching of scandium, aluminum and other valuable components from the non-magnetic tailings obtained from red mud after iron removal," *Metals (Basel).*, vol. 11, no. 3, p. 469, 2021.

[20] R. M. Rivera, B. Ulenaers, G. Ounoughene, K. Binnemans, and T. Van Gerven, "Extraction of rare earths from bauxite residue by dry digestion followed by water leaching," Miner. Eng., vol. 119, pp. 82–92, 2018, doi: 10.1016/j.mineng.2018.01.023.

[21] C. R. Borra, B. Blanpain, Y. Pontikes, K. Binnemans, and T. Van Gerven, "Recovery of rare earths and other valuable metals from bauxite residue (red mud): A review," *J. Sustain. Metall.*, vol. 2, no. 4, pp. 365–386, 2016, doi: 10.1007/s40831-016-0068-2.

[22] H. Li, J. Eksteen, and E. Oraby, "Recovery of rare earth elements from red mud by selective leaching: A review," Hydrometallurgy, vol. 185, pp. 127–139, 2019, doi: 10.1016/j.hydromet.2019.02.018.

[23] M. Ochsenkühn-Petropulu, T. Lyberopulu, and G. Parissakis, "Selective leaching of rare earth elements from red mud," Anal. Chim. Acta, vol. 296, no. 3, pp. 305–313, 1994, doi: 10.1016/0003-2670(94)80212-7.

[24] J. Vind *et al.*, "Rare earth element phases in bauxite residue," *Minerals*, vol. 8, no. 2, p. 77, 2018, doi: 10.3390/min8020077.

[25] T. Chen and others, "Hematite-to-magnetite transformation in microwave fields and its implications for magnetic separation," *Sep. Purif. Technol.*, 2016.

[26] J. Zhou, M. Dai, Q. Guan, H. Zeng, W. Sun, and L. Wang, "Optimizing the Dealkalization Process of Red Mud: Controlling Calcium Compounds to Improve Solid–Liquid Separation Performance," *Minerals*, vol. 15, no. 2, 2025.

[27] B. Hui *et al.*, "Sediment-Hosted Rare-Earth Elements Mineralization from the Dian--Qian District, Southwest China: Mineralogy and Mode of Occurrence," *Minerals*, vol. 14, no. 9, p. 903, 2024.

[28] H. Supriadi, S. Suyanti, W. Astuti, T. Handini, V. S. H. Sujoto, and G. Prameswara, "Optimization and Kinetics of Terbium Leaching from Lapindo Mud using Sulfuric Acid as the Leaching Agent," *Bull. Chem. React. Eng. \& Catal.*, vol. 20, no. 1, pp. 35–43, 2025.

[29] M. Mittermüller, J. Saatz, and B. Daus, "A sequential extraction procedure to evaluate the mobilization behavior of rare earth elements in soils and tailings materials," *Chemosphere*, vol. 147, pp. 155–162, 2016, doi: 10.1016/j.chemosphere.2015.12.079.

[30] Ruyters, S., Mertens, J., Vassilieva, E., Dehandschutter, B., Poffijn, A., & Smolders, E. (2011). The red mud accident in Ajka (Hungary): Plant toxicity and trace metal bioavailability in red mud contaminated soil. *Environmental Science & Technology*, 45(4), 1616–1622. https://doi.org/10.1021/es104000m.

[31] Z. Li. Toward low-carbon construction: a review of red mud utilization in cementitious materials and geopolymers for sustainability and cost benefits, Buildings, 16 (2026), 10.3390/buildings16020362.